processes

MDPI

Article

Influence of Soil Particle Size on the Temperature Field and Energy Consumption of Injected Steam Soil Disinfection

Zhenjie Yang [1], Adnan Abbas [1], Xiaochan Wang [1,2,*], Muhammad Ameen [1], Haihui Yang [1] and Shakeel Ahmed Soomro [1,3]

[1] College of Engineering, Nanjing Agricultural University, Nanjing 210031, China; 2016212010@njau.edu.cn (Z.Y.); dr_adnan219@yahoo.com (A.A.); 2016212014@njau.edu.cn (M.A.); 2019212004@njau.edu.cn (H.Y.); ssoomro@sau.edu.pk (S.A.S.)

[2] Jiangsu Province Engineering Laboratory for Modern Facilities Agricultural Technology and Equipment, Nanjing 210031, China

[3] Department of Farm Structures, Sindh Agriculture University, Tandojam 70060, Pakistan

* Correspondence: wangxiaochan@njau.edu.cn; Tel.: +86-25-58606567

Received: 20 December 2019; Accepted: 17 February 2020; Published: 20 February 2020

Abstract: Soil steam disinfection (SSD) technology is an effective means of eliminating soil borne diseases. Among the soil cultivation conditions of facility agriculture in the Yangtze River Delta region of China, the clay soil particles (SPs) are fine, the soil pores are small, and the texture is relatively viscous. When injection disinfection technology is applied in the clay soil, the diffusion of steam is hindered and the heating efficiency is substantially affected. To increase the heating efficiency of SSD, we first discretized the continuum model of Philip and De Vries into circular particle porous media of different sizes and random distribution. Then with Computational Fluid Dynamics (CFD) numerical simulation technology, a single-injection steam disinfection model for different SP size conditions was constructed. Furthermore, the diffusion pattern of the macro-porous vapor flow and matrix flow and the corresponding temperature field were simulated and analyzed. Finally, a single-pipe injection steam disinfection verification test was performed for different SP sizes. The test results show that for the clay soil in the Yangtze River Delta region of China, the test temperature filed results are consistent with the simulation results when the heat flow reaches H=20cm in the vertical direction, the simulation and test result of the heat flow in the maximum horizontal diffusion distance are L=13cm and 12cm, respectively. At the same disinfection time, the simulated soil temperature change trend is consistent with the test results, and the test temperature is lower than the simulated temperature. The difference between the theoretical temperature and the experimental temperature may be attributed to the heat loss in the experimental device. Further, it is necessary to optimize the CFD simulation process and add the disintegration and deformation processes of soil particle size with the change of water content. Furthermore, the soil pores increase as the SP size increases and that a large amount of steam vertically diffuses along the macropores and accumulates on the soil surface, causing ineffective heat loss. Moreover, soil temperature distribution changes from oval (horizontal short radius/vertical long radius = 0.65) to irregular shape. As the SP size decreases, the soil pore flow path becomes fine; the steam primarily diffuses uniformly around the soil in the form of a matrix flow; the diffusion distance in the horizontal direction gradually increases; and the temperature distribution gradually becomes even, which is consistent with the soil temperature field simulation results. Similar to the energy consumption analysis, the maximum energy consumption for SP sizes>27mm and <2mm was 486and 477kJ, respectively. Therefore, proper pore growth was conducive to the diffusion of steam, but excessive pores cause steam to overflow, which increased energy consumption of the system. Considering that the test was carried out in an ideal soil environment, the rotary tiller must be increased for fine rotary tillage in an actual disinfection operation. Although large particles may appear during the rotary tillage process, an appropriate

number of large particles contributes to the formation of a large pore flow, under the common effect of matrix flow, it will simultaneously promote greater steam diffusion and heating efficiency. The above theoretical research has practical guiding significance for improving the design and disinfection effect of soil steam sterilizers in the future.

Keywords: soil steam disinfection; soil particle size; soil temperature; soil water content; energy consumption

1. Introduction

Soil borne diseases caused continuous soil cropping problems and affect crop yield and quality. Soil physical disinfection technology is one of the important methods to prevent and control soil-borne diseases [1–4]. As compared to chemical methods, soil physical disinfection methods are clean, efficient, and environment friendly. Soil physical disinfection methods mainly include injected soil steam disinfection (SSD) method, flame disinfection method, solar energy disinfection method, and microwave disinfection method [1–8]. The flame disinfection method can generate a high temperature of 1000 °C in a short time. The high temperature of the flame is then directly sprayed to the ground for disinfection, this avoids the loss of heat during transmission, but does not entirely kill the harmful bacteria in deep soil. At the same time, high temperature eliminates the effective water in the soil and changes the physical properties of the soil. The flame disinfection method can achieve good disinfection effect in sandy soil, but is not appropriate for heavy red, clay and silt soil to heavy red soil, clay soil, and silt soil [1–4]. Furthermore, the solar energy disinfection method is pertinent with the areas having abundant heat resources, it is highly operable and is low in cost, but constrained by external factors such as weather and season [1,2]. The microwave disinfection method has a disadvantage of high operation cost and complicated operations when disinfecting soil [1,2]. The injection SSD method comparatively has a unique "evaporation–condensation" mechanism, which can effectively remove the condensed water blocked in the soil pores, promote the rapid diffusion of steam, and improve the heating efficiency of the soil by steam [6–8]. The injected SSD method can effectively kill harmful bacteria in the deep soil. At the same time, high temperature steam can also humidify the soil to change the pellet structure and restore the pellet activity [6–8]. Earlier the application of soil steam disinfection technology has some problems, like high steam disinfection cost and heavy boiler weight [9], which demoted the wide use of soil steam disinfection technology among the farmers. However, in recent years, the cultivation of high-value-added crops has also encountered problems of continuous cropping, which severely affects its yield and quality, such as Panax notoginseng of precious Chinese medicine [10]. Compared with other disinfection methods, the soil steam disinfection method is the most effective and ecological method to overcome the obstacles of continuous cropping of Panax notoginseng [10]. Considering this problem and according to the characteristics of greenhouse cultivation of Panax notoginseng, Zhu designed a soil steam disinfection machine for Panax notoginseng [11]. At the same time, Pan's optimization and improvement of the soil steam sterilization boiler made the boiler and steam sterilizer smaller and more convenient to move [9]. Therefore, the steam disinfection technology will have more practical development prospects.

Although global experts have done a lot of studies on SSD boilers and machines, and the SSD efficiency has been greatly improved, there is still a need to explore the new methods to improve the disinfection efficiency, and the most essential thing for SSD is that this disinfection technology needs to be adapted to different soil types for disinfection. According to soil scientists, different soils have different contents of clay, silt, and sand. Due to the large sand content, the sandy loam has good gas permeability [12,13]. Clay loam or clay has significant clay contents with fine and small particles, resulting in poor gas permeability [12,13], especially the compacted soil produced after continuous cropping [14,15]. Hence, Gay [6] discovered that when steam is diffused in sandy loam soil, the soil heating rate increases as the soil water content (SWC) increases because sandy

loam soil promotes the diffusion of steam in soil due to its large pores [6,7]. The injected SSD method can reheat and remove condensed water that is blocked in the pores of sandy loam soil to promote the diffusion of steam in the soil [6]. However, most of the soil types of the Yangtze River Delta in China are clay or clay loam due to its high clay content and soil porosity. Small soil pores reduced water permeability and gas permeability [14,15]; removal of the condensed water blocked in the pores is difficult. Therefore, in the case of the injectable disinfection method for soil, the diffusion of steam is hindered, which caused a decrease in the heating efficiency of the soil and an increase in the energy consumption, which affects SSD performance. During the actual cultivation process, the clay produced by the compaction would have aggregates or soil blocks of different sizes, and then form pores of various sizes. Depending on the size of the soil pores, the flow of fluid in the soil can be divided into matrix flow (small pore flow or capillary flow) and large pore flow [16,17], as shown in Figure 1a. When large numbers of large pores exist in soil, fluid rapidly crosses the soil particles (SPs) along the large pore channels to form a large pore flow. In clay or clay loam, which is more viscous, the large pore flow generated by the macropores may help to accelerate the flow of gases and liquids and increase the aeration of the soil relative to the matrix flow [16,17]. Especially in the process of SSD, proper pore growth is beneficial to increase the diffusion speed and range of steam. However, excessive soil pores may cause steam to spread too quickly on the surface of soil and overflow into the atmosphere, which caused ineffective heat loss. Eventually, the interior of the large soil particles or clods cannot be completely heated to the required temperature. Therefore, in the process of steam disinfection, it is necessary to change the compacted large soil clods into small particles to promote the rate and range of soil heating by steam.

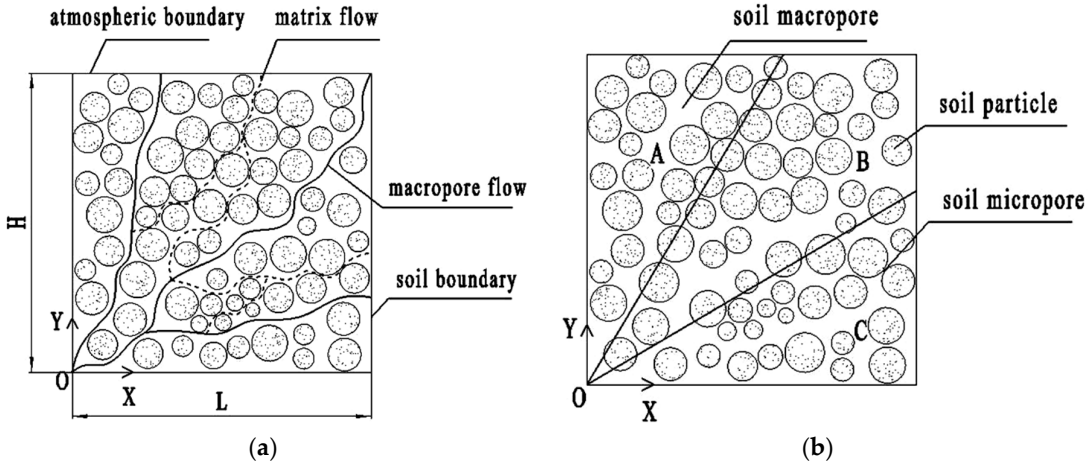

Figure 1. Schematic of steam heat transfer in large pores. (**a**) soil pore diagram; (**b**) heat transfer zone. Note: Point O is the heat source point of the steam, and L and H represents the horizontal and vertical diffusion distance of the steam heat flow.

When the compacted large soil clods become small soil particles and small clods, the form and direction of the flow during the steam disinfection process will also change. According to previous studies on the flow of liquid water in large pores, it was shown that liquid water mainly used large pores as the diffusion center, and diffused downward in a radial divergence along with small pores. However, for the steam disinfection process, the diffusion and flow direction of steam in large and small pores are uncertain. The areas where steam may diffuse are represented as A, B, and C. Figure 1b depicts the following possible scenarios: if the horizontal velocity is less than the vertical velocity, the steam is concentrated in the A region; if the horizontal velocity is equal to the vertical velocity, the vapor diffusion is concentrated in the B region; and if the horizontal velocity is greater than the vertical velocity speed, the steam is concentrated in the C area.

In order to explore the diffusion direction and range of the steam heat flow under different soil particle size conditions, based on the research by Philip and De Vries, according to the actual soil particle size and pore width range, the media model is discretized into circular particles of different

sizes and randomly distributed porous media. The SP size (<2 mm) after fine soil rotary tillage was used as the control group; and four SP sizes (>27 mm, 17–27 mm, 7–17 mm and 2–7mm) were set as the test groups. Using CFD numerical simulation technology, a single-pipe injection steam disinfection model under different soil particle sizes was constructed, and the diffusion forms of the large-pore steam flow and matrix flow and the corresponding temperature fields were simulated and analyzed to determine the steam disinfection area. Based on the temperature field simulation, the single-pipe injection type soil steam disinfection test was mainly performed. This paper determined the use of three kinds of steam flow rates under different disinfection durations. The effects of 5 soil particle sizes on soil temperature, water content, and energy consumption were mainly analyzed.

2. TheoreticalAnalysis

2.1. Selection of Soil Macropore Model

To facilitate the solution of the soil heat transfer equation, most of the soil models areconsidered to be continuous homogeneous porous media [18]. However, after actual cultivation, the soil has particle sizes and pores of different sizes. To further explore the variation in the single-injection soil temperature (*ST*) of a field in different SP size conditions, a suitable large pore soil model needs to be selected and determined. Currently, specialists from various countries do not provide a strict definition of large pores in the soil. Beven believes that a preferential flow of large pores exists when the pore width is greater than 0.3 cm [19,20]. Luxmoore and Lamande defined pores with a width greater than 0.1 cm as macropores [21,22], while Singh et al. utilized image processing methods to study soil macropores and set the lower limit width of macropores to 0.16 cm [23]. To determine the range of pore widths that corresponds to SPs and soil block diameters (referred to as SP diameters), first, the compacted soil produced by actual continuous cropping obstacles needs to be smashed by rotary cultivation and the SPs and soil blocks are sieved using a test sieve. According to previous research results [19–23], in this paper, the SP size<2 mm is set as the control group and the soil block particle sizes are divided into four levels (2–7 mm, 7–17 mm, 17–27 mm, and >27 mm) as shown in Figure 2. Each group of soil samples was subjected to five repeated sieving treatments. The collected soil was subjected to an image processing analysis, and the pore widths that corresponded to different particle sizes were counted to determine a large-pore soil model.

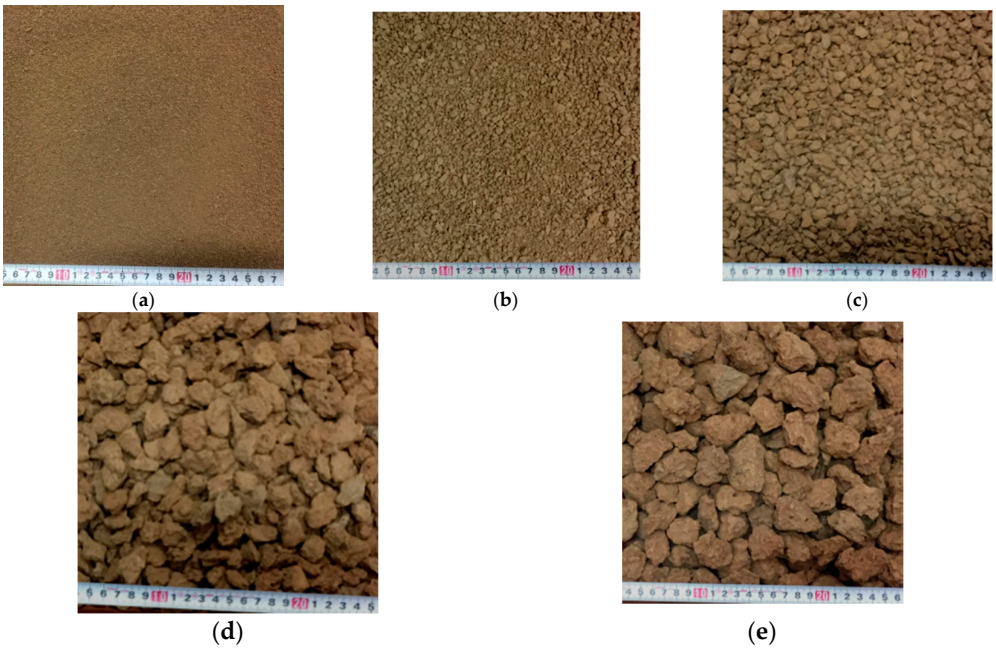

Figure 2. Soil pattern. (**a**)<2 mm; (**b**)2–7 mm; (**c**)7–17 mm; (**d**)17–27 mm; and (**e**)>27 mm.

This paper uses the set of measurements to analyze particles by Image J software (1.8.0, National Institutes of Health, Bethesda, MD, USA, 2020), obtain and calculate the porosity and pore channel width of the soil layer in the same plane as the steam disinfection pipe (SDP) [24–26]. The morphological characteristics of pores treated with different particle sizes are shown in Table 1 and Figure 3. Some differences exist in the definition of macropores by domestic and foreign experts. According to Singh and Luxmoore et al. [21–23], the width of the pore channel in the particle size section 2–7 mm is between 0.068 and 0.172 cm, and the particle size section is in the transition zone between large pores and small pores. The width of the pore channel in the particle size section 7–17 mm is between 0.13 cm and 0.33 cm, and the particle size section is a large pore area. According to Beven et al.'s definition of the lower limit of soil macropores, pores with a width greater than 0.3 cm are macropores [19,20]. As shown in Table 1, the width of the pore channel in the particle diameter section 17–27 mm is between 0.43 cm and 0.91 cm, and the particle size section is a large pore area. The width of the pore flow channel with a particle size section >27 mm is between 0.46 and 1.56 cm, and the particle size section is in a large pore area.

As shown in Table 1 and Figure 3, as the particle size decreases, the soil porosity gradually decreases. However, the number of small pores gradually increases, and the distribution becomes more uniform. With a small particle size and small pores, obtaining a loose and porous soil structure is beneficial. As the size of the soil clod increases, the width of the soil pore channel gradually increases. Compared with soil with a small particle size and small pores, steam will preferentially flow out of large pores. Although large pores increase the aeration of soil, they also increase the diffusion rate of steam to the soil surface. Excessive soil pores cause steam to diffuse directly to the soil surface, which requires additional steam to heat deep soil during the disinfection process. The steam collected on the soil surface will simultaneously overflow into the air, which causes an ineffective loss of steam heat.

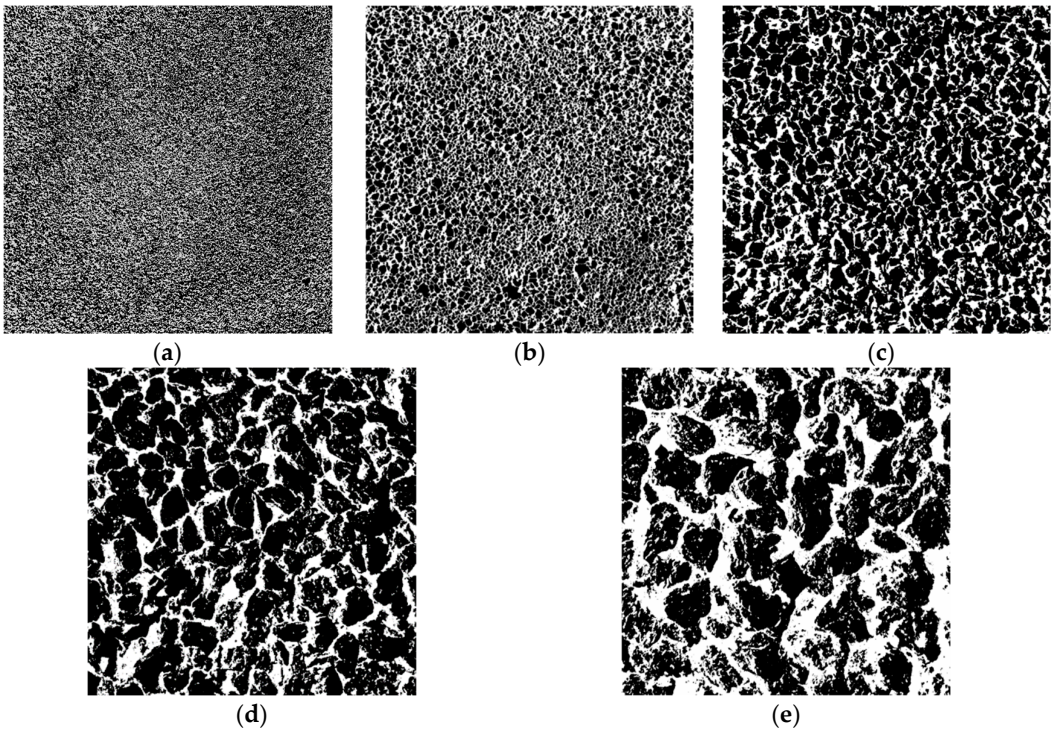

Figure 3. Two-dimensional vertical profile of soil pore. (**a**) <2 mm; (**b**) 2–7 mm; (**c**) 7–17 mm; (**d**) 17–27 mm; and (**e**) >27 mm. Note: The black parts represent soil particles (SPs) or clods, and the white parts represent pores.

Table 1. Soil porosity and pore width.

SP Diameter/cm	<2 mm	2–7 mm	7–17 mm	17–27 mm	>27 mm
porosity/%	39.02 ± 0.83	40.14 ± 0.56	41.43 ± 1.20	44.02 ± 1.35	47.05 ± 1.52
pore width/cm	0.048 ± 0.024	0.12 ± 0.052	0.23 ± 0.10	0.67 ± 0.24	1.01 ± 0.55

Note: Data are the mean ± standard deviation.

2.2. Establishment of a Soil Macropore Model

The shape of the natural SPs extensively varies, and a distinct dividing line among the particles does not exist. In soil science, SPs or soil blocks are generally simplified into spheres. Therefore, in this paper, the homogeneous soil in the study area is separated into equivalent circles of different sizes. The diameter of a circular particle is referred to as the SP diameter, and pore channels of different sizes are formed among particles. A simplified model of discrete soil is established using geometric modeling tools in COMSOL Multiphysics software (5.4, COMSOL Inc, Stockholm, Sweden, 2020). The SDP hole (heat source point) is shown in Figure 4. According to the determination of the soil size and pore width range, particle sizes <2 mm, 2–7 mm, 7–17 mm, 17–27 mm, and >27 mm are randomly generated in a 200 mm × 200 mm square soil area. The atmospheric boundary is set as a thermal insulation layer, and the heat exchange between the soil and outside air can be disregarded, as shown in Figure 4a,c,e,g,i. In this paper, a quadrilateral mesh is created for the model. The number of mesh elements is approximately 280,000, and the number of mesh nodes is approximately 57,000 as shown in Figure 4b,d,f,h,j.

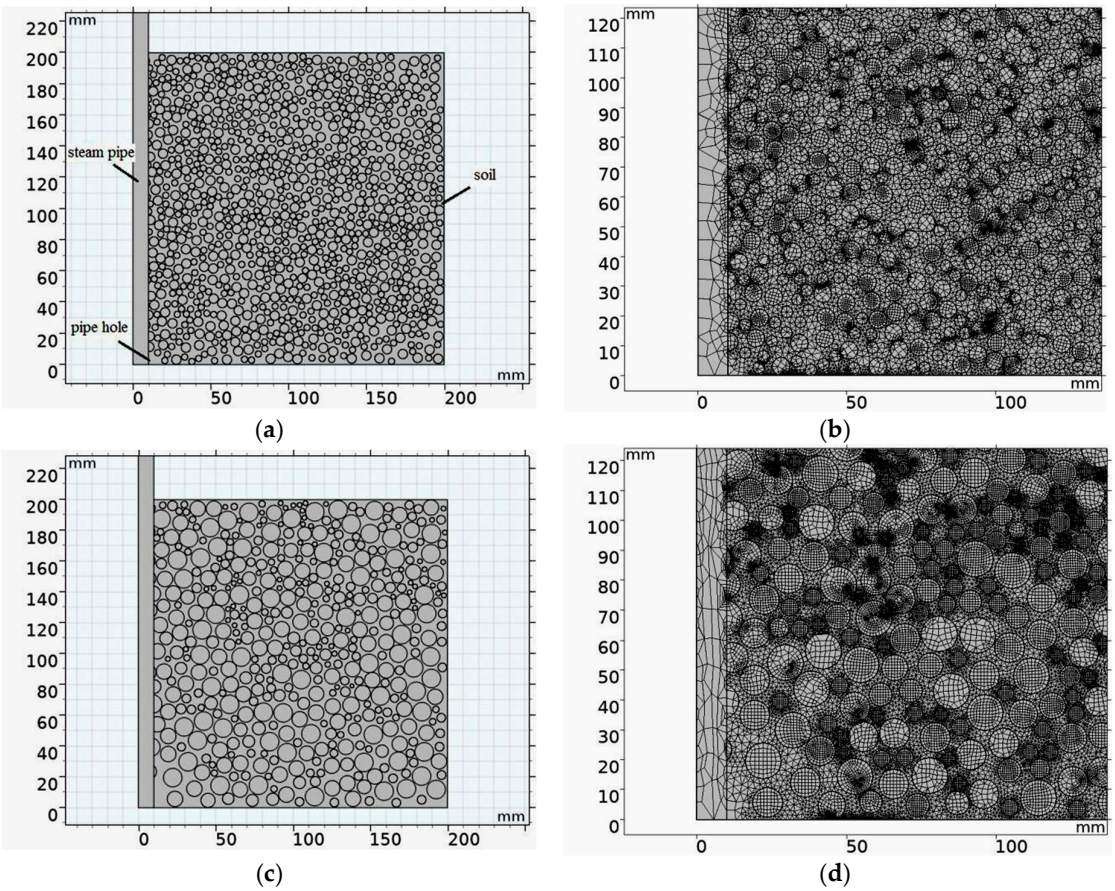

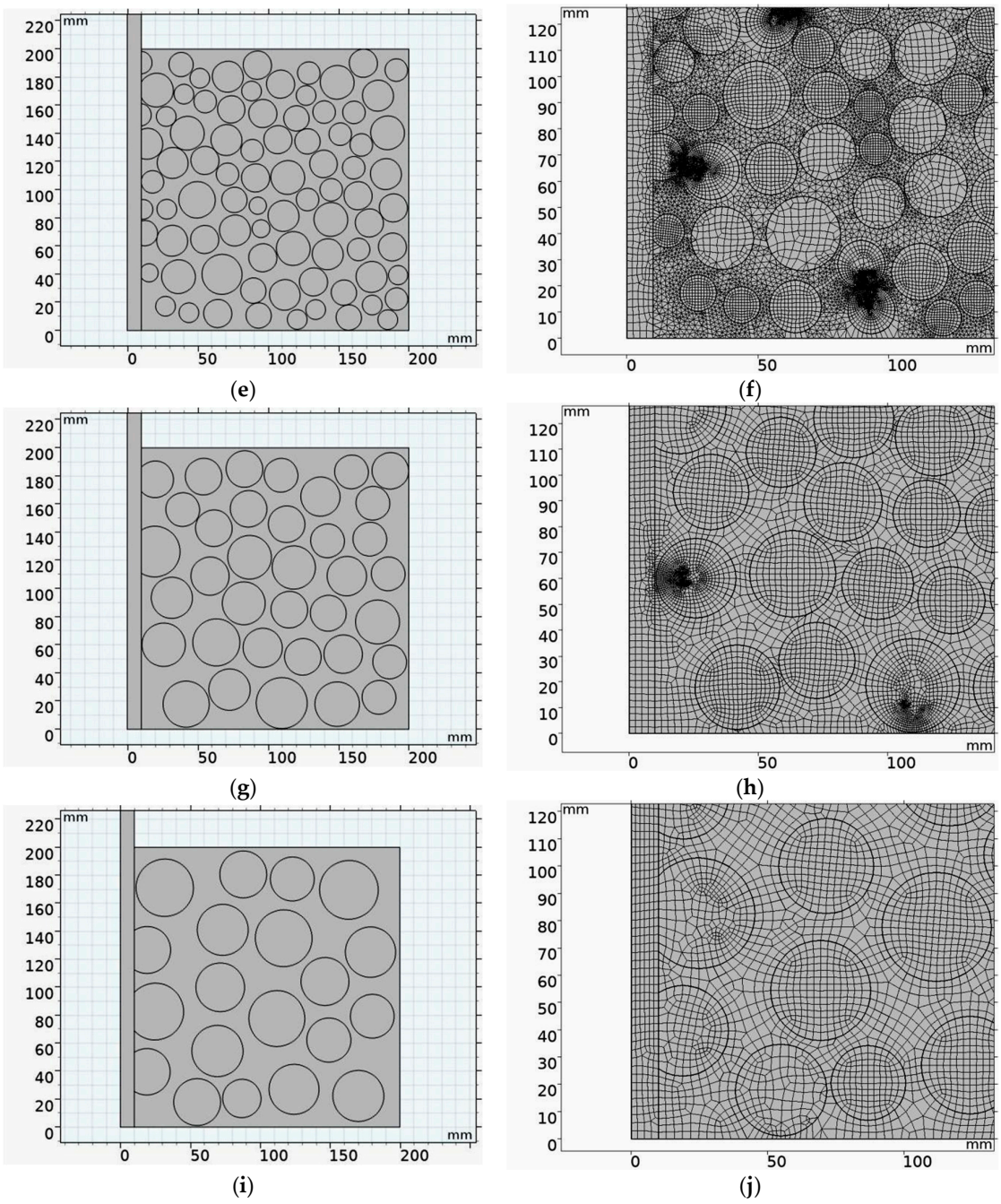

Figure 4. Steam disinfection model. (**a**) <2 mm model; (**b**)<2 mm meshing; (**c**) 2–7 mm model; (**d**)2–7 mm meshing; (**e**) 7–17 mm model; (**f**) 7–17 mm meshing; (**g**) 17–27 mm model; (**h**) 17–27 mm meshing; (**i**) >27 mm model; and (**j**) >27 mm meshing. Note: The meshing figures are partially enlarged views.

The heat transfer equation is numerically calculated according to Equations (1) and (2). Refer to Table 2 for the soil physical properties. Due to a large number of disinfected capillary pipes in actual operation, the steam flow rates of single tubes are set to 2, 3, and 4 kg/h. According to previous research, the steam temperature is set to 130 °C; the physical properties of the fluid (air and steam) are shown in Table 3.

Table 2. Soil physical parameters.

ST/°C	Soil Bulk Density/(kg/m³)	Soil Particle Density/(kg/m3)	Specific Heat/(J/(kg·K))	Soil Particle Diameter/mm	Porosity
20	1150	1005	1700	<2 mm	0.39
				2–7 mm	0.41
				7–17 mm	0.42
				17–27 mm	0.45
				>27 mm	0.49

Table 3. Fluid parameters.

Air Temperature /°C	Air Density/(kg/m³)	Air Specific Heat/(J/(kg·K))	Steam Temperature/°C	Steam Density/(kg/m³)	Steam Specific Heat/(J/(kg·K))
20	1.205	1005	130	1.497	2176.3

In this paper, the *ST* field is numerically simulated using the heat transfer equation of porous media proposed by De Vries [27]. The expression is as follows:

$$(\rho C_p)_{eff} \frac{\partial T}{\partial t} + \rho C_p \cdot u \cdot \nabla T + \nabla \cdot q = Q \quad (1)$$

$$(\rho C_p)_{eff} = \theta_p \rho_p C_{\rho,p} + (1-\theta_p)\rho C_p \quad (2)$$

whereρ_p is the soil bulk density, kg/m³; $C_{\rho,p}$ is the soil specific heat capacity, J/(kg·K); C_p is the fluid heat capacity at constant pressure, J/(kg·K); T is the absolute temperature, k; u is the velocity, m/s; q is the conducted heat flux (W/m²); Q is the additional heat source (W/m³); $(\rho C_p)_{eff}$ is the effective volumetric heat capacity at constant pressure defined by an averaging model to account for both the solid matrix and the fluid properties, J/(m³·K); and $1 - \theta_p$ is the porosity.

2.3. Analysis of Simulation Results

Based on the analysis of the homogeneous soil temperature field in the previous section, the effect of steam temperature on the soil heating rate is small and the effect of steam flow on the soil heating rate is large. Table 4 shows that under the same steam temperature condition, as the steam flow rate increases, the disinfection time used when the steam heat flux reaches the soil surface layer (SS treatment) and when the steam is completely filled with soil (SA treatment) gradually decreases.

Table 4. Soil steam disinfection (SSD)time.

Type	Steam Temperature/°C	Steam Flow/(kg/h)	Disinfection Time s
SS treatment	130	2	300
	130	3	220
	130	4	165
SA treatment	130	2	460
	130	3	310
	130	4	230

Note: SS treatment means that the steam just reaches the surface of the soil, and SA treatment means that the steam is completely filled with soil.

This article primarily analyzes the single-SDP injection temperature field, treated with a steam flow of 2 kg/h. As shown in Figures 5a–d, the treatments with particle sizes <2 mm and 2–7 mm are consistent with the shape of the temperature distribution of the homogeneous soil and the range of

high temperature (above 80 °C). For disinfection for 300 s, the high-temperature area was distributed in the middle and lower layers in a 1/4 ellipse. When the diffusion range of the steam heat flow in the vertical direction was H = 0–−20 cm, the diffusion distance in the horizontal direction was L = 13 cm. At the end of the disinfection, the high-temperature area gradually became rectangular, and the surface soil appeared "overheated". As shown in Figure 5e, during the 300 s disinfection, the high-temperature area with a particle size of 7–17 mm is irregularly distributed in the upper and middle layers of the soil, which differs from the distribution of the high-temperature area with a particle size of <2 mm and 2–7 mm. When Singh and Luxmoore et al. investigated the soil macropores [21–23], all soil pores with a particle size segment <2 mm were small pores, the particle size segment of 2–7 mm was in the transition region between large and small pores, and the particle size segment of 7–17 mm was in the large pore area. Although the particle size section 2–7 mm is in the transition zone between large pores and small pores, as shown in Figures 5a–c, the steam heat flow treated with particle sizes <2 mm and 2–7 mm is uniform in the form of the matrix flow in the horizontal and vertical directions in the soil. The shape and distribution range of the two groups of particle diameters in the high-temperature area are equivalent, while the steam heat flow with particle diameters of 7 to 17 mm primarily diffuses to the soil surface in the form of large pore flows in the vertical direction (Figure 5e).

As shown in Figures 5e,g,i, in the large-pore treatment group with particle sizes of 7–17 mm, 17–27 mm, and >27 mm, larger soil block pores correspond to more irregular heat diffusion of steam, and a higher temperature also correspondsto more irregular heat diffusion of steam. The regular shape is concentrated in the soil pores, and the steam quickly diffuses around the soil large particles to the surface in the form of large pore flows in the vertical direction. When disinfecting for 300s, the diffusion range of the steam heat flow in the vertical direction was H = 0–−20 cm, and the diffusion distance in the horizontal direction was L=10–13cm.Comparing the particle diameters <2 mm and >27 mm, the steam with a particle size of less than 2 mm evenlydiffuses around the soil in the form of a matrix flow of small pores, while the steam with a particle size of >27 mm forms a large pore flow. In diffusion to the soil surface, the diffusion rate of the steam heat flow in the vertical direction gradually increases. For example, with a disinfection time of 300 s, the vertical distances in the high-temperature region with a particle size of <2 mm and a particle size of >27 mm are 140 mm and 190 mm, respectively.

Considering that the lethal temperature of the harmful bacteria is 80 °C [6], as shown in Figure 5 with the same disinfection time, the larger the particle size is, the smaller the distribution range of the high-temperature soil area, that is, the smaller the scope of the disinfection area. For example, the soil disinfection area with a particle size >27 mm is the smallest. In the treatment with a particle size >27 mm, the soil pores are the largest, and the steam is primarily diffused to the surface of the soil in the form of a large pore flow. Therefore, with the limited disinfection time (460 s), the temperature inside the soil block is significantly lower than the temperature of the steam in the pores. As the soil clod decreases, the internal temperature of the soil clod gradually approaches the pore temperature. At the end of the disinfection, the heat flow diffusion distance in the horizontal direction of each treatment is less than L = 15 cm.

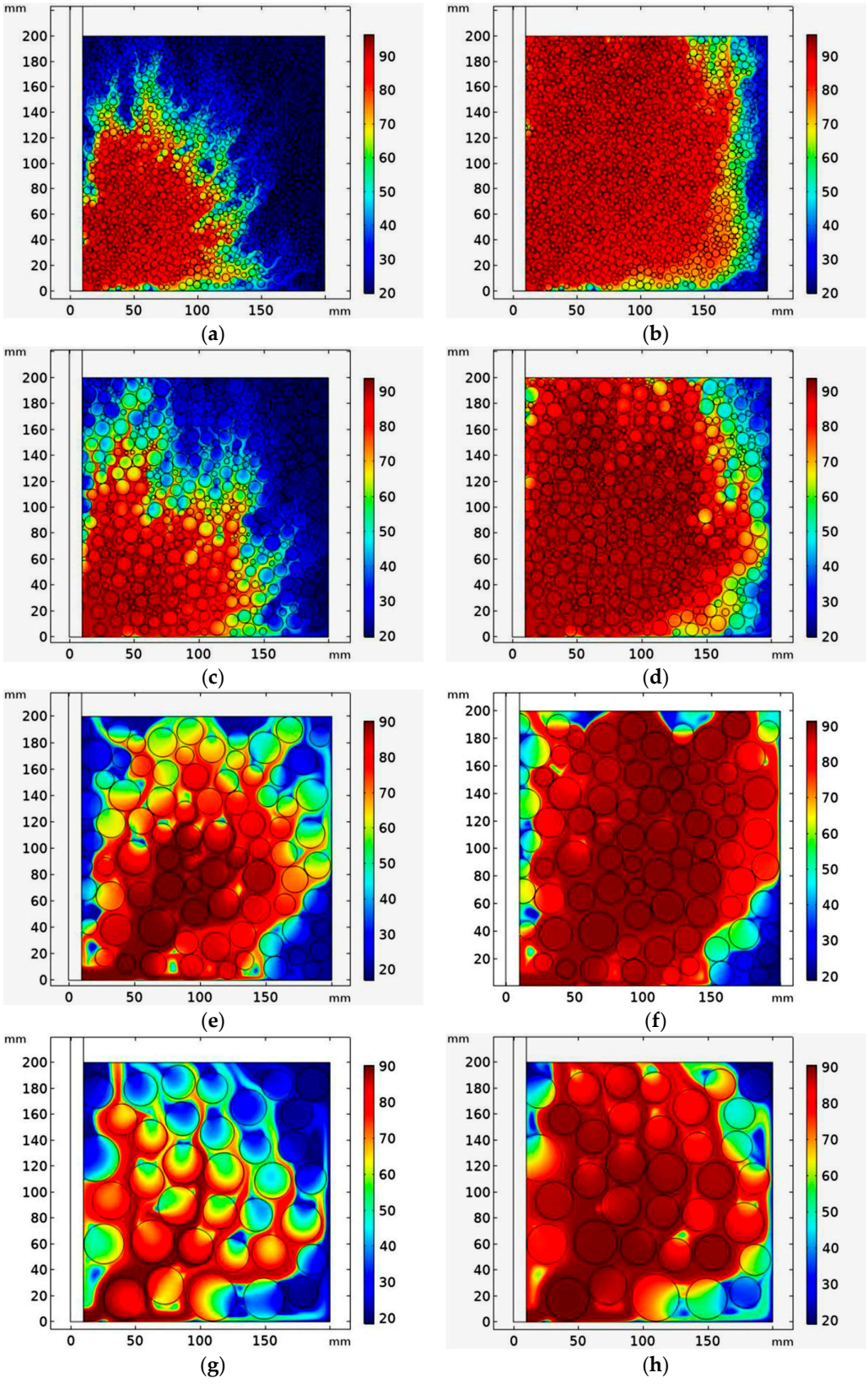
mm
200
180
160
140
120
100
80
60
40
20
0
0
50
100
150
mm
90
80
70
60
50
40
30
20

(**a**) (**b**)

(**c**) (**d**)

(**e**) (**f**)

(**g**) (**h**)

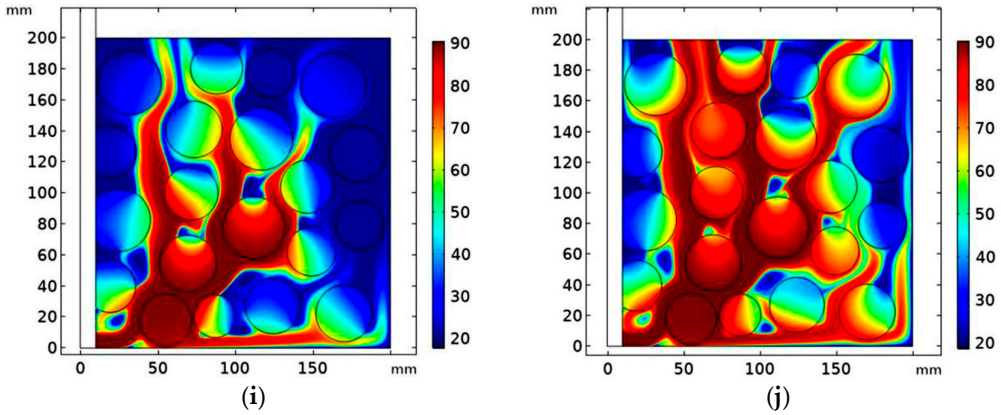

Figure 5. Soil temperature simulation results: (**a**) <2 mm, t=300s; (**b**)<2 mm, t=460s; (**c**) 2–7 mm model; (**d**)2–7 mm meshing; (**e**) 7–17 mm model; (**f**) 7–17 mm meshing; (**g**) 17–27 mm model; (**h**) 17–27 mm meshing; (**i**) >27 mm model; and (**j**) >27 mm meshing. Note: The legend indicates the ST/°C.

The average temperatures of the soil with different particle sizes and times of disinfection are shown in Figure 6. At the beginning of disinfection, the temperature increase rate of the particle sizes of 7–17 mm, 17–27 mm, and >27 mm is faster than that of the particle sizes of <2 mm and 2–7 mm. Because the pores are large, the steam quickly spreads to the various layers of the soil, and results in a higher heating rate. With the progress of disinfection, the heating rate of the particle diameters 7–17 mm, 17–27 mm, and >27 mm is gradually lower than that of the particle sizes for the 2–7 mm and <2 mm treatments. When disinfected for 400 s, the temperature of the particle sizes 2–7 mm and <2 mm exceeds 86 °C; the temperature of the particle sizes 7–17 mm and 17–27 mm can exceed 82 °C, and the minimum temperature of the particle diameter >27 mm is only 78 °C. A larger particle size corresponds to larger pores. Part of the steam heat is concentrated in the pores, and the temperature of the soil block is low. Part of the steam will quickly diffuse along with the large pores to the surface of the soil, which causes an ineffective loss of heat. As a result, the soil temperature is generally low. As shown in the analysis of the soil temperature map in Figure 6, the change in the heating curve of the particle diameters of <2 mm and 2–7 mm is almost constant. The temperature of the particle diameter of 7–17 mm is slightly higher than that of the particle diameter of 17–27 mm.

According to the analysis of the pore section, with the treatment of the small pore section and the large pore transition section with a particle diameter of <2 mm and 2–7 mm, that is, the treatment of pores less than 0.1 cm in diameter, the temperature field exhibits similar changes. The temperature is 80 °C, disinfection time is 300 s, the temperature of the SP diameters of <2 mm and 2–7 mm can exceed 80 °C, and the range of the effective soil disinfection area is the largest. Due to the different definitions of pores, the particle sizes of 7–17 mm, 17–27 mm, and >27 mm belong to the macropore section. However, the soil temperature rise curve, the particle size >27 mm treatment and the particle size of 7–17 mm reveal a large difference in the change in the temperature rise of the 17–27 mm treatment. The temperature of the particle diameter >27 mm treatment is lower than that of other particle diameter treatments. The pores of the particle diameter >27 mm treatment are excessive—between 0.46and 1.56 cm.A large amount of steam is unable to collect below the surface of the soil, and heat is lost from the soil surface to the air along with the large pores. For disinfection time =350 s, the temperature of the soil treated with particle sizes of 7–17 mm and 17–27 mm can reach 80 °C, which satisfies the lethal temperature of harmful bacteria [6]. At the end of the disinfection (460s), the temperature of the soil treated with particle size >27 mm is always lower than 80 °C and does not satisfy the lethal temperature of harmful bacteria [6], and the area of effective soil disinfection is the smallest.

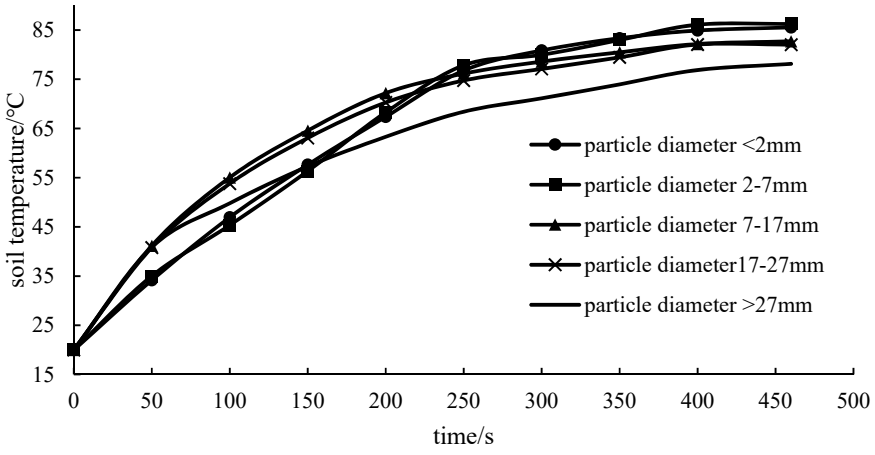

Figure 6. Temperature variation of different soil particle sizes.

3. Soil Steam Disinfection Test

3.1. Test Conditions and Materials

One SDP was tested, and it had a length of 300 mm, a diameter of 10 mm, and a wall thickness of 2 mm. One end of the SDP was the inlet end, and the other end was the closed end. Three holes (aperture = 3 mm) were uniformly distributed at a distance of 10 mm from the closed end, and the circumferential direction of the holes was 120°.

The test soil was obtained from the test base of the Yanhai Tractor Factory. The basic properties of the soil are shown in Table 5.

Table 5. Physical properties of soil.

Soil Types	Soil Particle Compositions/%		
	Clay (<0.002 mm)	Silt (≥0.002–0.02 mm)	Sand (≥ 0.02–2 mm)
Clay	53.3%	23.3%	23.3%

The SSD test bench is shown in Figure 7, and the test components and manufacturers are shown in Table 6.

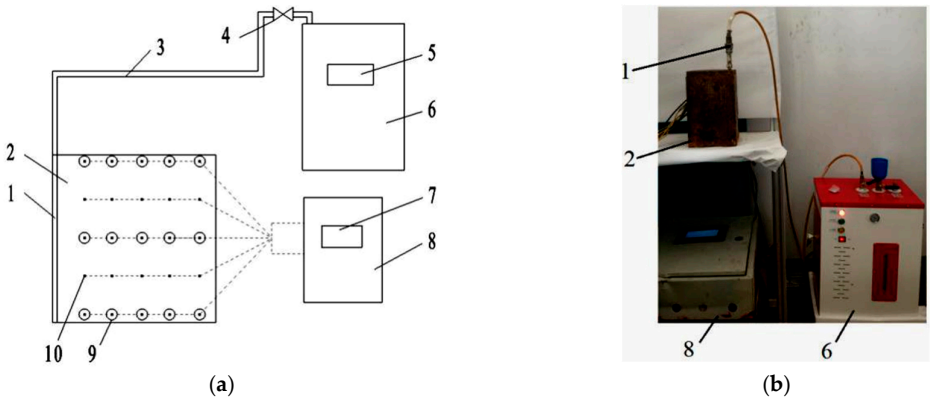

(**a**) (**b**)

Figure 7. Soil steam disinfection (SSD) test bench: 1. steam disinfection pipe; 2. soil trough; 3. steam transport pipe; 4. ball valve switch; 5. boiler pressure controller; 6. boiler; 7. control box screen; 8. soil temperature, water content control box; 9. Soil water content sensor; 10. Soil temperature sensor. (**a**) components of the SSD test bench; (**b**) SSD test.

Table 6. Test components and manufacturers.

Test Components	Manufacturer
JHD steam generator	Shangrao Jiangxin Boiler Co., Ltd., Shangrao, China
LYK-10 boiler pressure controller	Changzhou Liping Electronic Equipment Co., Ltd., Changzhou, China
Y60 pressure gauge	Hongsheng Instrument Factory Co., Ltd., Fuyang, China
Q911F flow valve	Nanjing Meiyue Valve Co., Ltd., Nanjing, China
LUGB-20 flow meter	Nanjing Lantewan Electronic Technology Co., Ltd., Nanjing, China
ST-SWC control box	/
Steam disinfection pipe	/
Soil bin (20 cm × 20 cm × 30 cm)	/
soil temperature sensor	Jinan Zhengmiao Automation Equipment Co., Ltd., Jinan, China
soil water content sensor	Jinan Zhengmiao Automation Equipment Co., Ltd., Jinan, China

3.2. Test Methods

According to the simulation and previous research results [6,13,15], the hardened soil was mashed and then the SP sizes were divided into 6 grades by using sieves of >27 mm, 17–27 mm, 7–17 mm, 2–7 mm, and <2 mm; and then the soil was loaded into the same volume of a test soil bin for the SSD test.

The initial soil temperature was (20.1 ± 2) °C, and the water content was (18 ± 2)%. The temperature sensor selected for the test was a thermocouple soil temperature sensor with a measurement range of 0–200 °C. The soil water content sensor was based on the principle of frequency domain reflection, and the measurement range was 0–100%. According to previous research by Gay [6], the location of the soil temperature sensor and soil water content sensor was shown in Figure 8 and soil temperature and water content control system collected test data every 10s. The following steps were implemented: the residual condensate in the SDP was drained before the test; the boiler pressure was adjusted to 0.3 MPa; the saturated dry steam temperature was increased to 132.88 °C; the flow valve opening through the flow meter was calibrated; and the steam flow was calibrated to 2, 3, and 4 kg/h. The SDP was inserted into test areas (depth= −20 cm) for different particle diameters [6,7], and the surface of the soil bin was sealed with an iron cover to prevent steam overflow. According to the theoretical and simulation calculations, the disinfection times of the flow rates of 2, 3, and 4 kg/h are set to 360, 240, and 180 s, respectively. The disinfection test ends with the statistics of the total amount of steam that flows through the flow meter *Qs*. Each group of experiments was repeated 3 times for a total of 45 groups.

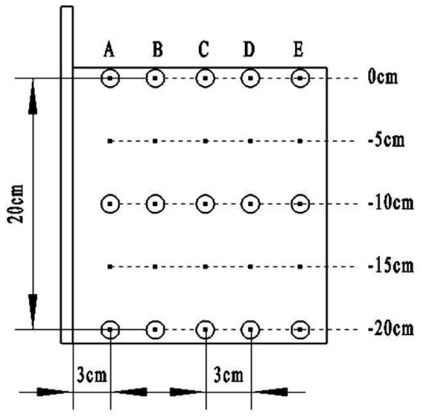

Figure 8. ST-SWC test layout. Note: The large circle represents the soil water content(SWC) sensor position, and the small circles represent the soil temperature (ST) sensor position.

3.3. Data Analysis

The *ST* rise rate is an important indicator used to measure the change in temperature. The rate is expressed as follows:

$$v_T = \frac{T_t - T_{t-1}}{\Delta t} \tag{3}$$

where V_T is the *ST* rise rate, °C/s; T_{t-1} is the *ST* at $t - 1$, °C; and Δt is the time interval between t and $t - 1$, s.

The *ST* coefficient of variation (*Cv*) can reflect the uniformity of the *ST* distribution. The smaller the temperature coefficient of variation is, the better the uniformity of the *ST* distribution. The *Cv* calculation formula is as follows:

$$Cv = \frac{SD}{\overline{X}} \tag{4}$$

where *SD* is the standard deviation of *ST*, °C, and $\overline{X}$ is the average *ST*, °C.

The energy consumption can reflect the degree of utilization of steam heat by the disinfection system. The calculation formula is as follows:

$$Ws = Q_s \cdot H \tag{5}$$

where Q_s is the cumulative amount of steam, kg; *H* is the enthalpy change in steam to liquid water, kJ/kg.

The vertical profiles of ST and SWC were plotted using Surfer 12 software (Golden Software, Inc.). The distributions of ST and SWC were obtained from the vertical profiles. The area that corresponds to the STs below 60 °C is the low-ST area; the area that corresponds to the STs of 60–80 °C is the moderate-ST area, and the area that corresponds to STs>80 °C is the high-ST area. In the figures, red represents the high-ST area; green and yellow represent the moderate-ST area, and blue and black represent the low-ST area. The area that corresponds to SWCs below 25% is the low-SWC area; SWCs of 25–30% correspond to the moderate-SWC area; and SWCs >30% correspond to the high-SWC area. In the figures, red represents the high-SWC area; green and yellow represent the moderate-SWC area, and blue and black represent the low-SWC area.

4. Results and Analysis

4.1. Analysis of the Change in Soil Temperature

The change in the soil average temperature and disinfection time is shown in Figure9. The temperature of soil heating is gradually accelerated in the initial stage of disinfection because the temperature difference between steam and soil is large at the initial stage of disinfection and the heat transfer is sufficient. In the later stage of disinfection, the soil temperature field tends to be stable. As indicated by the simulation analysis, the variation law of the temperature rise curve with the particle diameters of <2 mm and 2–7 mm is the same.

Given the same particle size condition, with an increase in the steam flow rate, the soil heating curve shifts to the left; the slope of the curve gradually increases; the temperature of the soil heating increases; and the time required for the soil to heat to the same temperature decreases. Similar to soil remediation techniques, increasing the aeration flow can increase the efficiency of contaminant removal and shorten the soil remediation time. For the same flow rate, with a decrease in the SP size, the largest value of the soil average temperature gradually increases and the temperature for the treatment of <2 mm particles can exceed 80 °C.

Comparing the results of Figure 9b with the simulated and test temperature, it can be seen that the trend of the soil temperature rise curve is basically the same. At the same disinfection time, the test temperature is lower than the simulated temperature. For example, the theoretical simulation and actual soil temperature of disinfection for 360s, particle size <2mm, flow rate 2kg/h are 85.3 °C and 81.4 °C, respectively, and the test temperature is slightly lower than the theoretical simulation temperature. The difference between the theoretical temperature and the experimental temperature may be attributed to the heat loss in the experimental device.

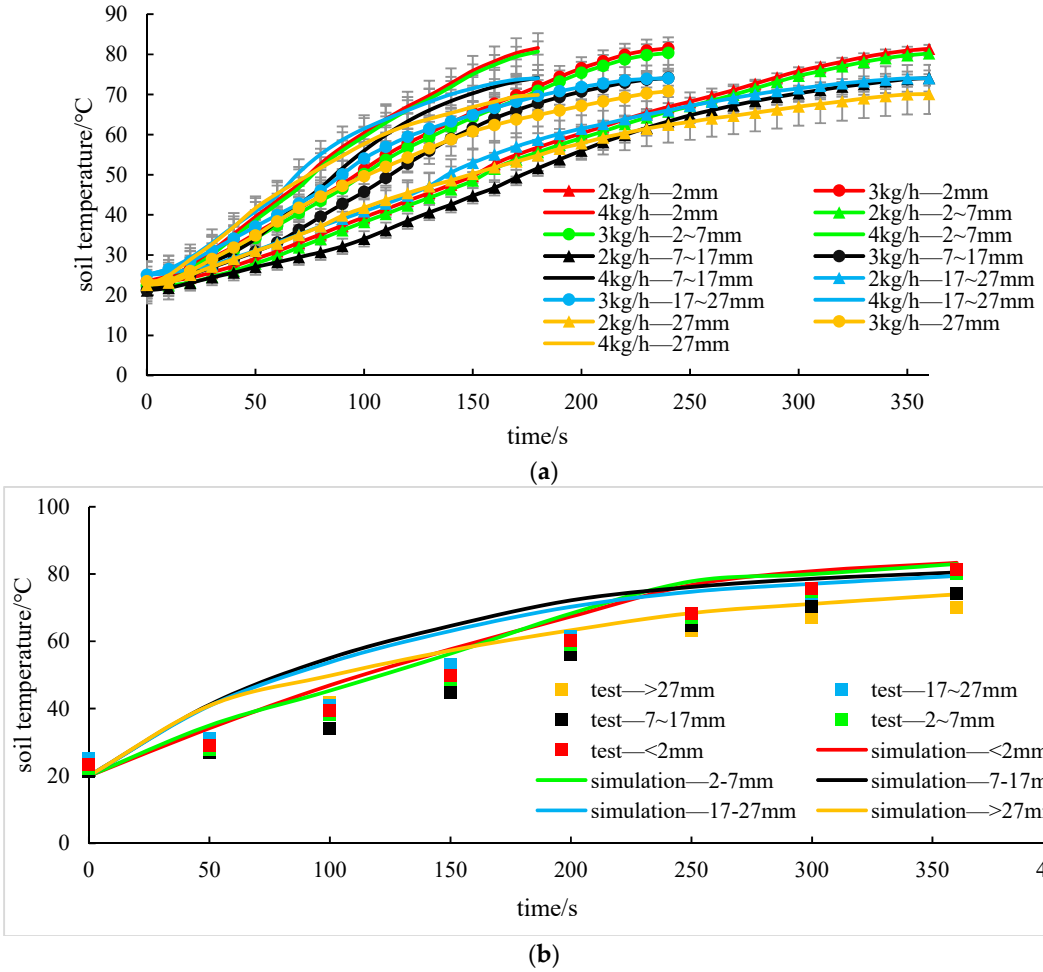

Figure 9. Mean *ST* with time. (**a**) Soil temperature-time change under different flow and particle size test conditions; (**b**) Soil temperature-time simulation and experimental comparison of different particle size conditions at a flow rate of 2kg/h. Note: 2 kg/h-2 mm means that the steam flow of the treatment group is 2 kg/h, and the particle size of the soil is <2 mm. The same conditions apply in the following section.

As shown in Figure10, the average temperature rise rate and time curve of the soil show a parabolic change, and the slope of the curve before the peak is larger than the slope of the curve after the peak; that is, the curve rapidly rises to the peak and then gradually decreases and reaches a stable value. At the same flow rate, the peak temperature rise rate in the 27 mm diameter treatment corresponds to a considerably shorter disinfection time than other treatments, because a large particle size corresponds to a large pore width, and the steam quickly fills the entire flow path. Thus, the soil heating rate is faster. However, as the disinfection time is extended, the soil temperature field gradually stabilizes. At the same spacing, the larger is the steam flow rate, the higher is the

starting point of the curve, and the higher the peak temperature of the soil heating rate, which is consistent with the trend of the average soil temperature and disinfection time.

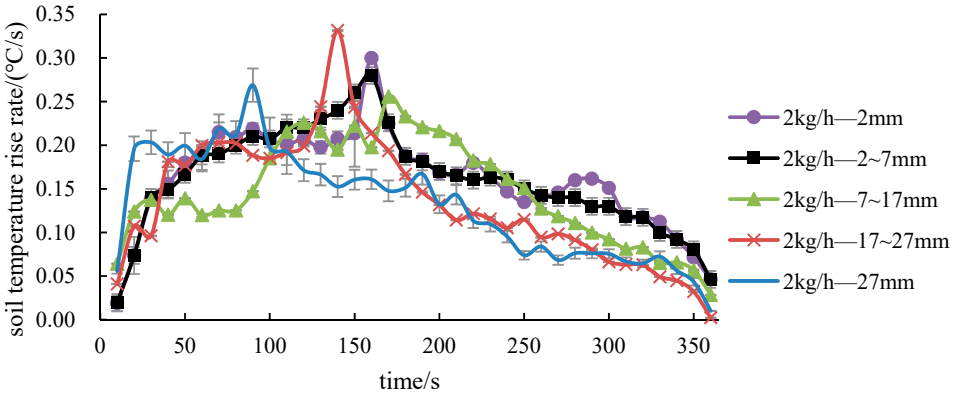

(**a**)

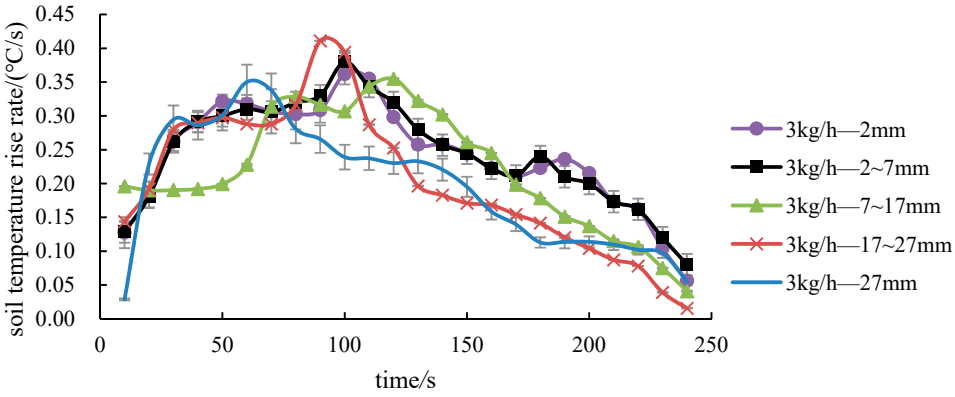

(**b**)

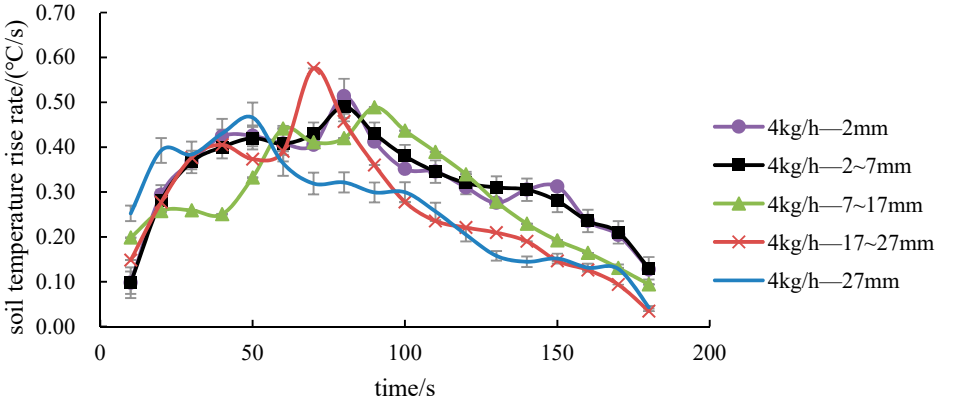

(**c**)

Figure 10. Variation in mean *ST* rise rate and disinfection time. (**a**) 2 kg/h; (**b**) 3 kg/h; and (**c**) 4 kg/h.

4.2. Soil Temperature Distribution Analysis

As shown in Figure 11, the soil temperature coefficient of variation and the time curve show a parabola change, and the slope of the peak front curve is larger than the slope of the peak curve. The soil temperature at the pipe hole is too high due to the initial stage of disinfection. The total temperature difference is large, and the temperature distribution is not uniform. The soil temperature field tends to be stable in the late stage of disinfection, the temperature difference is

gradually reduced, and the temperature distribution is uniform compared with the early of disinfection period. Similar to the analysis of the simulated temperature field, the magnitudes of temperature change with the particle diameters of <2 mm and 2–7 mm are the same.

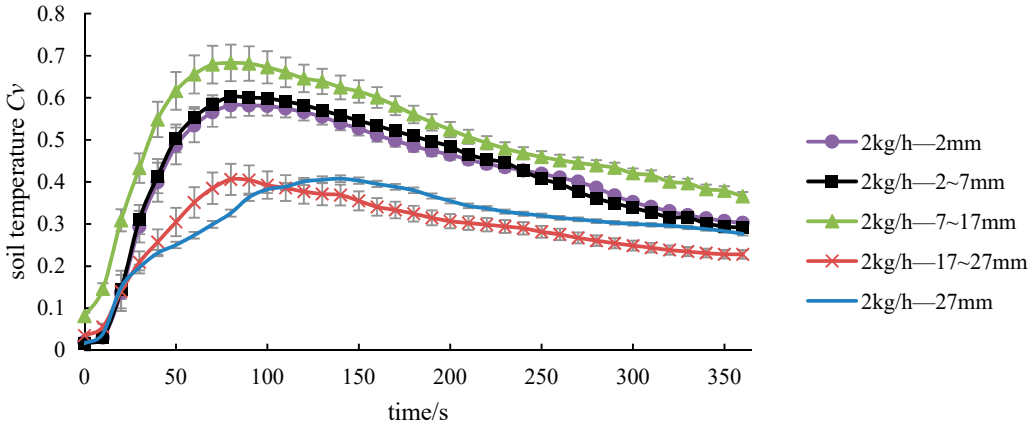

(a)

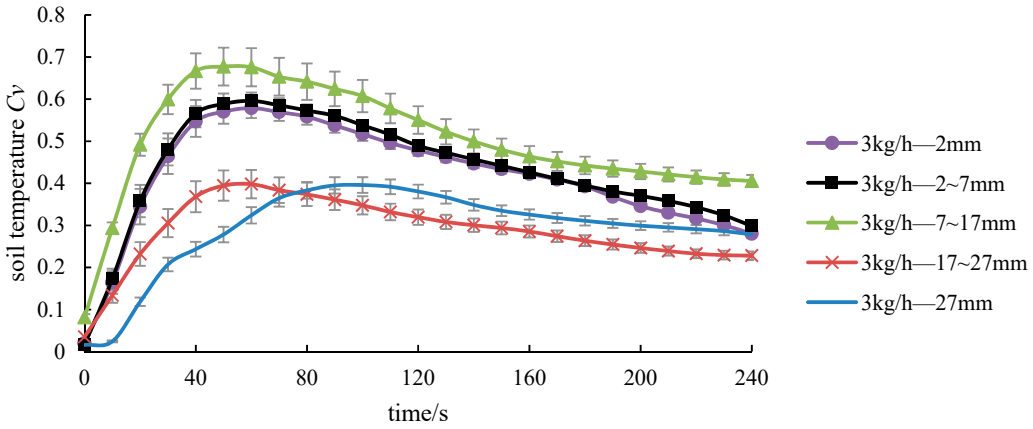

(b)

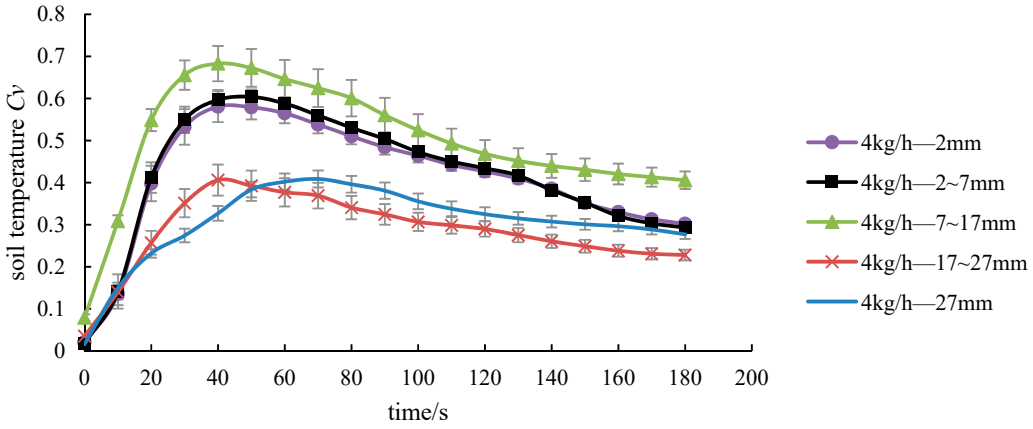

(c)

Figure 11. Variation in the mean *ST* variation coefficient with disinfection time. (**a**) 2 kg/h; (**b**) 3 kg/h; and; (**c**)4kg/h.

At the same flow rate, the temperature variation ranges of particles with diameters of 2 mm and 2–7 mm is basically consistent and the curves for particle with sizes >27 and 17–27 mm were lower than those for the particle with sizes of 7–17, 2–7 and <2 mm. However, as the disinfection progressed, the curve with a particle size of <2 mm gradually decreased and approached that of the particles with sizes of >27 and 17–27 mm, which was based on an analysis of the rate of temperature increase. When the particle size of the soil is large, the steam quickly fills the soil; thus, the soil temperature distribution is relatively uniform. When the small particle size soil has small pores, the steam slowly spreads around the soil in the initial stage of disinfection. However, with the progress of disinfection, the temperature distribution gradually becomes uniform. For the same particle size conditions, the soil temperature coefficient of variation curves for different flow rates were the same, which indicated that the soil temperature changes of the same particle size treatment were the same for different flow rates.

Due to the different flow rates, the soil temperature distribution of the same particle size is the same and the temperature distribution of the particles with sizes of <2 mm and 2–7 mm is basically the same. Therefore, this chapter primarily analyzes the soil layer temperature for the condition of the flow rate of 2 kg/h and particle size treatments of < 2 mm, 7–17 mm, 17–27 mm, and >27 mm.

As shown in Figure 12 a, b, the temperature rise curves for the particle sizes <2 and 2–7 mm are similar. The deeper temperature rise rate of the soil is higher than that of the soil surface. The maximum deep temperature of the soil is 105 °C, and the maximum surface temperature is 99 °C, which indicates that the deep layer of the soil is directly heated by high-temperature steam. Further, this finding indicates that the heat transfer method is primarily thermal convection, which is the same as that obtained by Gay in the gas phase [6]. As shown in Figure 12 a, b, the temperature of the soil heating at point E is lower than that of other test points at the end of the disinfection, and the temperature is only 40 ± 10 °C, while the temperature of each layer of soil at test points A–C can exceed 70 °C. This finding indicates that the steam level is heated from 0 to 9 cm when the steam is heated to the soil surface (0 cm).

Comparing Figure 12a and Figure 12b, Figure 12c,d reveal that the temperature rise in the middle and surface layers of the soil is higher than that in deep soil, and the maximum surface temperature of the soil is 90 °C, which indicates that in the large pore flow, the steam directly passes over the soil and the heat transfer method is primarily heat convection. Since the steam heat is concentrated on the surface of the soil to form a superheated area, the temperature of the deep soil will decelerate [6]. As shown in Figure 12 c, d, the soil temperature at each test point is sequentially increased, and the soil heating rate at point E at the end of disinfection is lower than that for other test points. This finding indicates that steam can rapidly diffuse around the soil in large pores but the horizontal diffusion range is less than 15 cm.

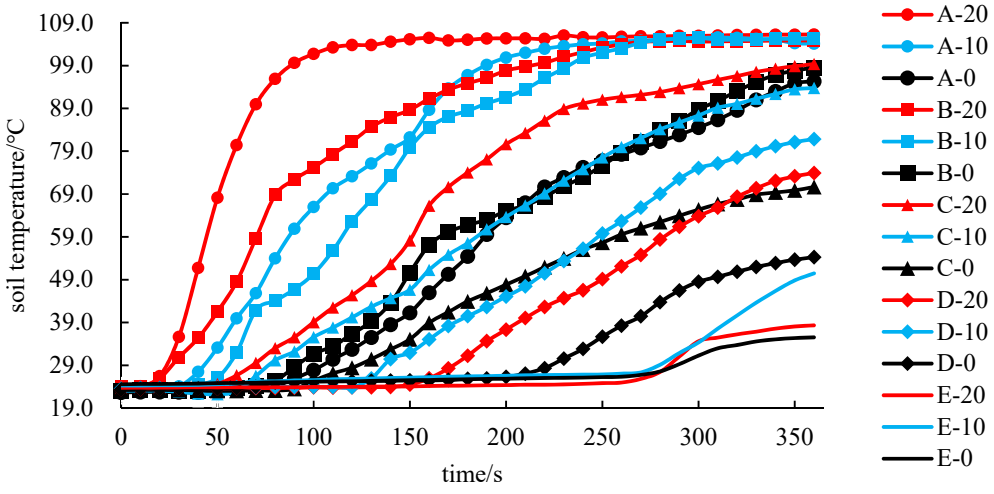
soil temperature/°C
109.0
99.0
89.0
79.0
69.0
59.0
49.0
39.0
29.0
19.0
0
50
100
150
200
250
300
350
time/s
A-20
A-10
A-0
B-20
B-10
B-0
C-20
C-10
C-0
D-20
D-10
D-0
E-20
E-10
E-0

(**a**)

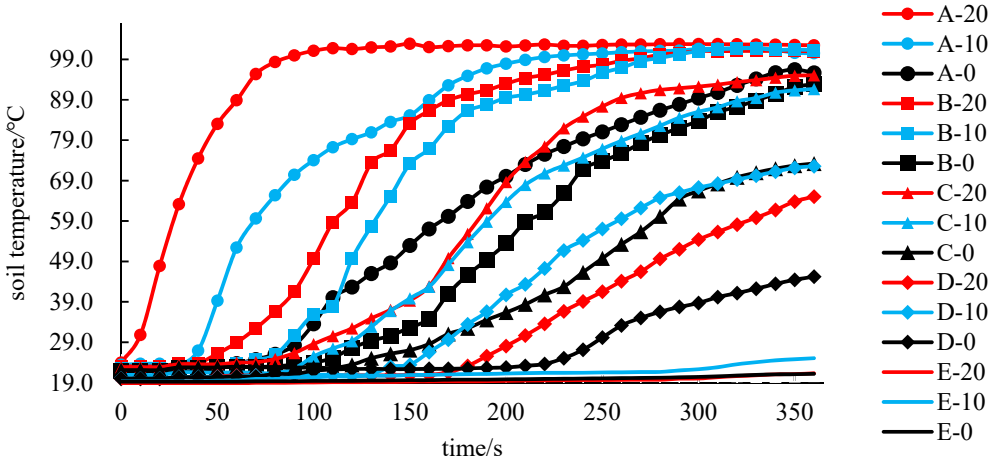
soil temperature/°C
99.0
89.0
79.0
69.0
59.0
49.0
39.0
29.0
19.0
0
50
100
150
200
250
300
350
time/s
A-20
A-10
A-0
B-20
B-10
B-0
C-20
C-10
C-0
D-20
D-10
D-0
E-20
E-10
E-0

(**b**)

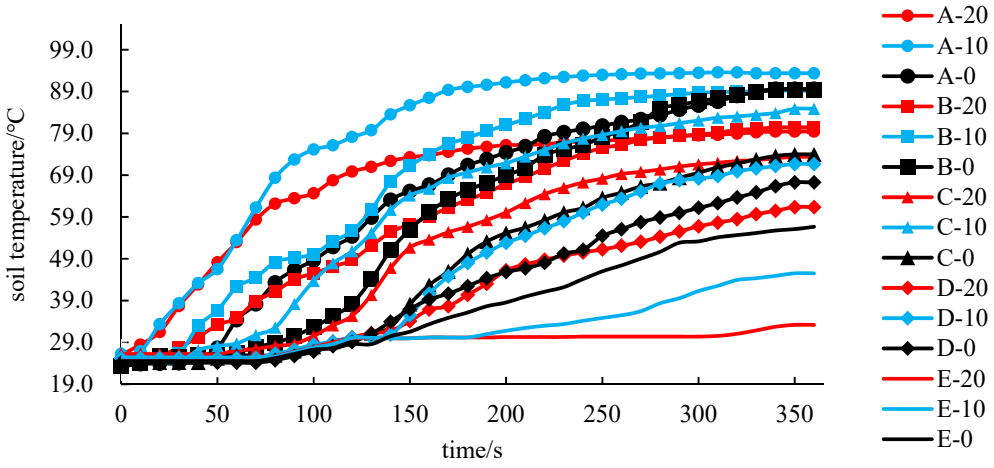
soil temperature/°C
99.0
89.0
79.0
69.0
59.0
49.0
39.0
29.0
19.0
0
50
100
150
200
250
300
350
time/s
A-20
A-10
A-0
B-20
B-10
B-0
C-20
C-10
C-0
D-20
D-10
D-0
E-20
E-10
E-0

(**c**)

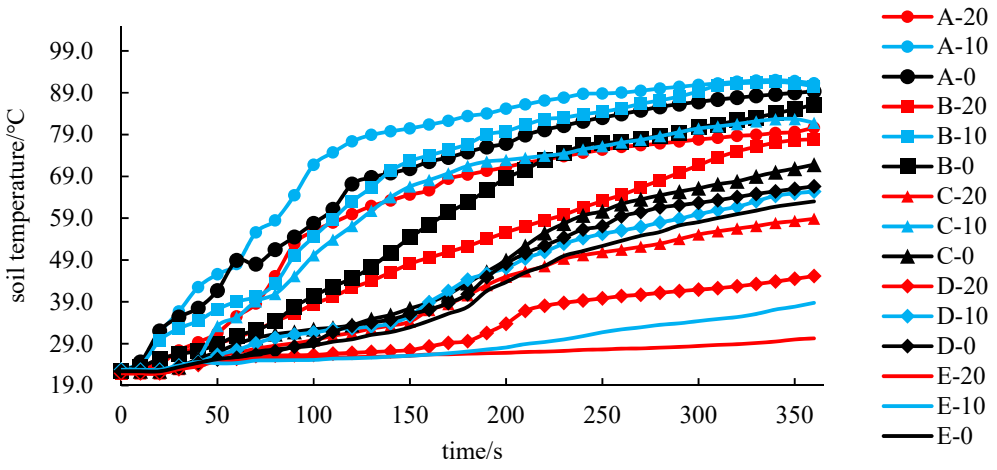

(**d**)

Figure 12. Variation diagram of *ST* and disinfection time in each layer: (**a**) <2 mm; (**b**) 7–17 mm; (**c**) 17–27 mm; (**d**) >27 mm. Note: A-20 indicates that A is the test point, and 20 is the test depth (−20cm). The same conditions apply in the following section.

As shown in soil temperature distribution profile in Figure 13, the particle sizes are 2 and 7–17 mm. At the beginning of the disinfection, the high-temperature region in the soil is 1/4 elliptical (horizontal short radius: vertical long radius = 0.63) and is concentrated in the soil. In the deep layer (−20 cm), the soil temperature distribution is uneven; as the disinfection progresses, the steam gradually spreads around the soil, the surface temperature gradually increases, and the soil temperature distribution uniformity is improved. When disinfected for 300 s to 360 s, the soil high-temperature area changes from oval to rectangular distribution that is concentrated in the horizontal direction (*L*) of 0–12 cm and the vertical direction (*H*) of 0–−20 cm. For the particle sizes are 17–27 and >27 mm, at the beginning of the disinfection, the high-temperature region in the soil is 1/2 elliptical (horizontal short radius: vertical long diameter = 0.41) and primarily distributed in the upper layer of soil (−5–−14 cm). When disinfected for 300 s to 360 s, the high-temperature zone of the soil is 1/4 elliptical and concentrated in the horizontal direction of *L* = 0–10 cm and vertical direction of *H* = 0–−20 cm, and the deep layer of the soil is located in the middle and low temperature zone (below 80 °C). The thermal range of single-SDP steam is concentrated in the horizontal *L* = 9–12 cm and vertical *H* = 0–−20 cm, which is consistent with the simulation results.

For the same disinfection time, as the soil pores increase, the high-temperature region gradually migrates to the soil surface. The smaller the particle size of the soil is, the greater the thermal interaction distance of the steam in the horizontal direction. For example, the particle size is 2 mm, and the maximum steam horizontal heat action distance is 12 cm. A larger SP size corresponds to a larger thermal interaction distance of the steam in the vertical direction. For example, when the particle size is >27 mm and the disinfection time is 240 s, the surface layer of the soil gradually appears in the high-temperature region (above 80 °C). Therefore, the larger the particle size is, the larger the soil pores, and the steam can be unobstructed along with the large pores. The steam spreads to the surface layer of the soil and accumulates on the surface of the soil to form a high-temperature area, which is consistent with the simulation results.

As shown in Figure 13, when the soil is disinfected for 240 s, the surface temperature that corresponds to the particle size of 2 mm does not exceed 80 °C and is primarily located in the middle and low temperature areas. When the soil is disinfected for 300 s, the surface layer of each treated soil begins to appear in the high-temperature area, such that a superficial area is formed in the surface layer of the soil. Due to the late stage of disinfection, the steam of each treatment primarily diffuses in the vertical direction and accumulates on the surface layer of the soil. Most of the heat begins to accumulate on the surface of the soil, and a small amount of heat may be lost to the air,

which is an ineffective loss of heat. At the end of the disinfection, the surface temperature of the soil with the particle sizes >27 and 17–27 mm is lower than that with the particle sizes 7–17 and 2 mm.

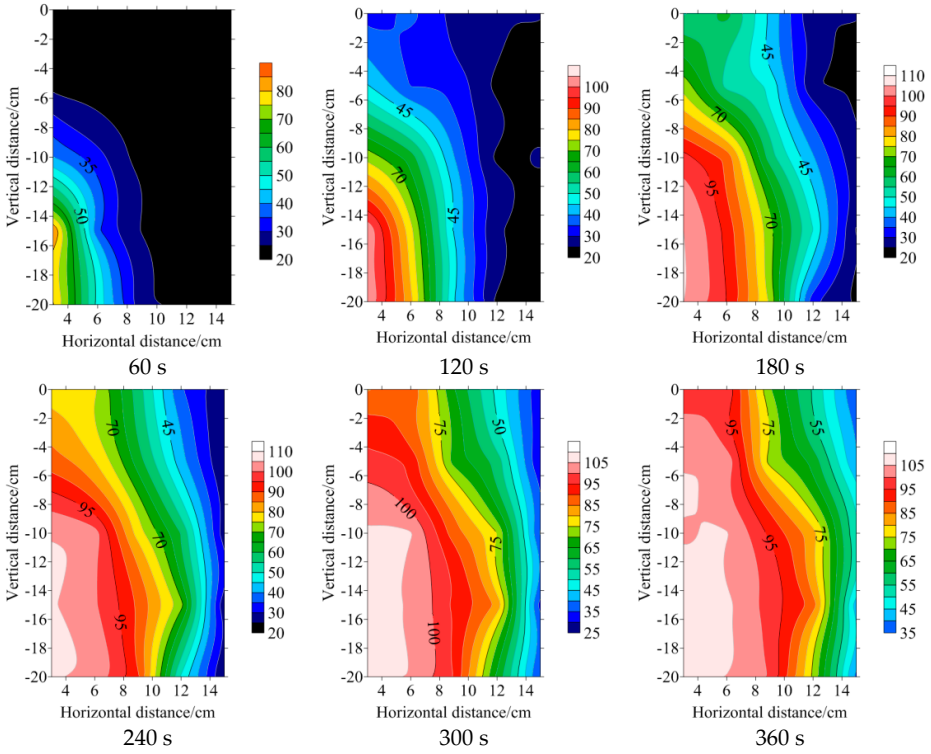

(**a**)

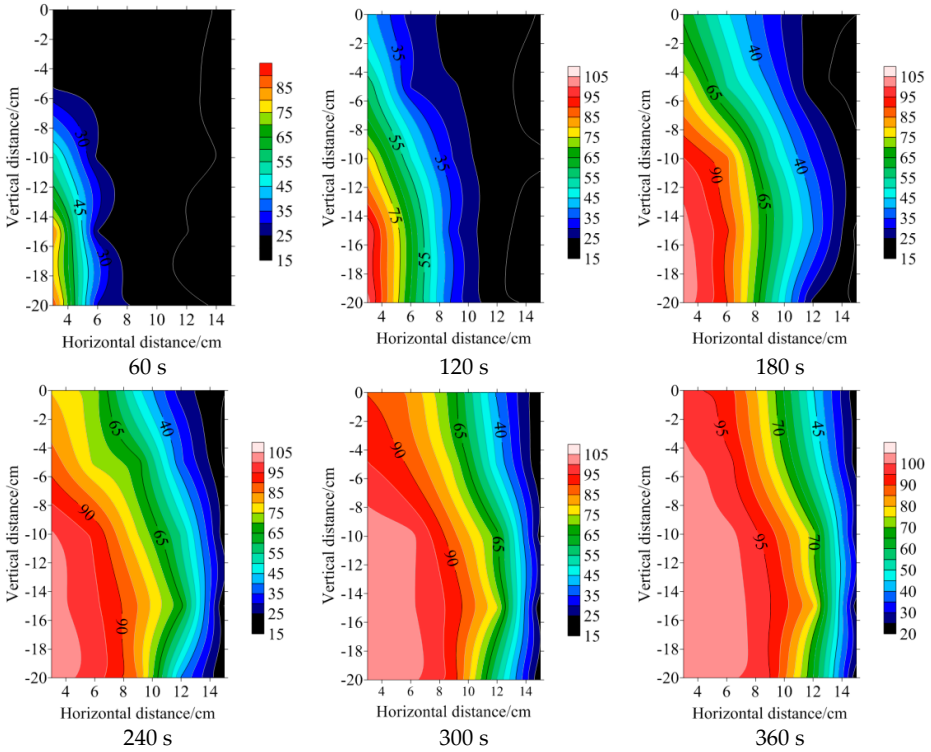

(**b**)

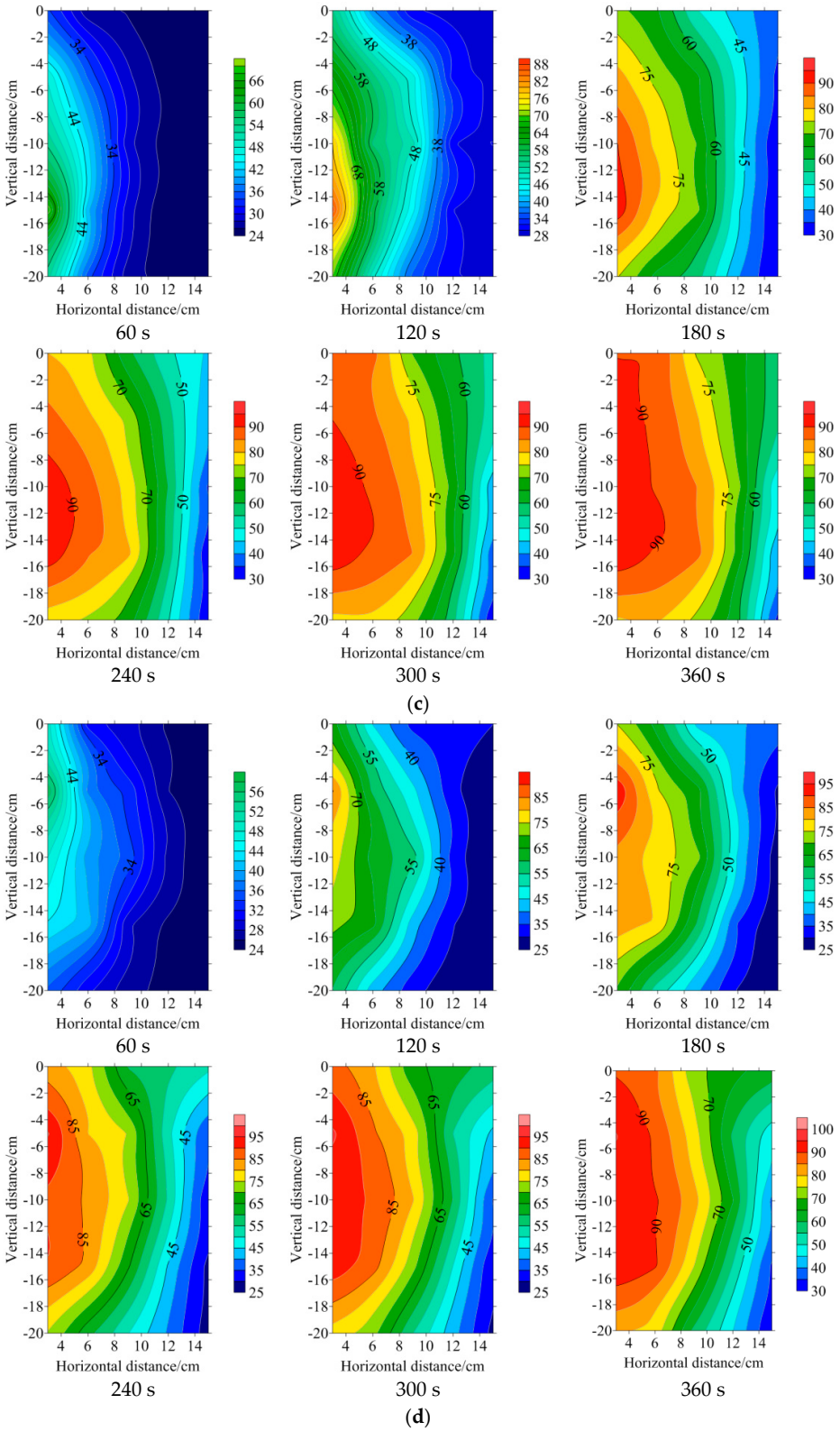

Figure 13. ST distribution: (**a**) <2 mm; (**b**) 7–17 mm; (**c**) 17–27 mm; (**d**) >27 mm. Note: The legend indicates the ST/°C and 60 s means that the disinfection time (*t*) is 60 s, 360 s means the disinfection time is 360 s, etc. The same conditions apply in the following section.

4.3. Soil Water Content Distribution Analysis

The soil water content distribution map reveals the diffusion law of steam. The heat transfer mode of each stage in the injection steam disinfection process is investigated in combination with the soil temperature distribution map.

As shown in the wetting front of the soil water content distribution profile 14, the particle sizes are 2 and 7–17 mm. At the beginning of the disinfection, the steam spreads around the soil in the form of a 1/4 oval shape, and the diffusion range is 0 to 11 cm in the horizontal direction. The straight direction is −2–−20 cm; at the end of disinfection, the middle and high water content areas are rectangular at the horizontal level of 0–13 cm and vertical level of 0–−20 cm; and the high water content area is concentrated in deep soil. When the particle sizes are 17–27 and >27 mm, the steam diffuses in the form of 1/2 ellipse. The diffusion range is 0–10 cm horizontally and 0—20 cm vertically. At the end of disinfection, the medium-high water content area is 1/4 oval. The horizontal level is 0–12.5 cm, and the vertical level is 0–−20 cm. The high water content area is concentrated in the upper layer of the soil. The diffusion range of single-SDP steam is concentrated at the horizontal level of 10–13 cm and the vertical level of 0–−20 cm.

For the same disinfection time, as the number of soil pores increase, the high water content region gradually migrates to the soil surface. In the initial stage of disinfection, a smaller SP size corresponds to a greater change in the horizontal water content than the vertical water content; thus, the steam primarily diffuses horizontally, such that the soil surface is in the middle and low water content areas. A larger SP size corresponds to greater water changes in the vertical direction; thus, the steam primarily diffuses vertically, and the deep layer of soil is in the middle and low water content area. The larger the particle size is, the larger the soil pores, and the form of steam flow is primarily large pore flow, such that the steam can be unobstructed along the large pores. The steam diffuses to the surface of the soil and accumulates on the surface of the soil. The smaller the particle size is, the smaller the pores of the soil. Consequently, the form of steam flow is primarily the matrix flow and a small part of the large pore flow, and the diffusion ability of steam in the horizontal direction is enhanced.

As shown in Figure 14, when the soil was disinfected for 60 s, the surface soil that corresponds to the particle sizes >27 and 17–27 mm has begun to appear in the middle water content area, while the surface soil that corresponds to the particle sizes 7–17 and 2 mm remains in the low water content area. When the soil was disinfected for 300 s, the steam with the particle sizes of 7–17 and 2 mm began to diffuse into the surface of the soil, such that the vertical diffusion speed was enhanced, and the vapor diffusion gradually became uniform. When the soil was disinfected for 360 s, the surface layer of each treated soil formed a high water-bearing area with a high content of >27 and 17–27 mm particle sizes. The water volume area is larger than that of the area with particle sizes of 7–17 and 2 mm.

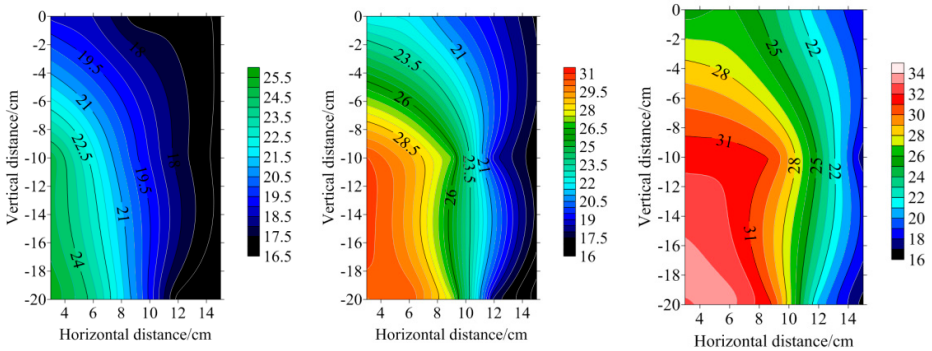

60 s 120 s 180 s

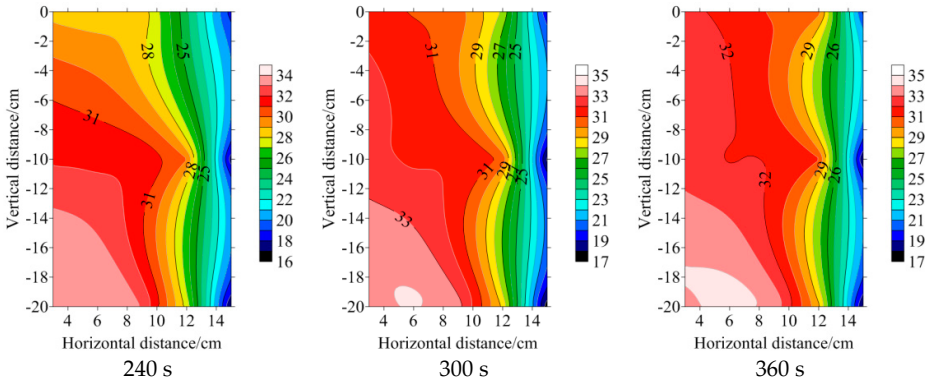
Vertical distance/cm
Horizontal distance/cm
240 s
300 s
360 s

(**a**)

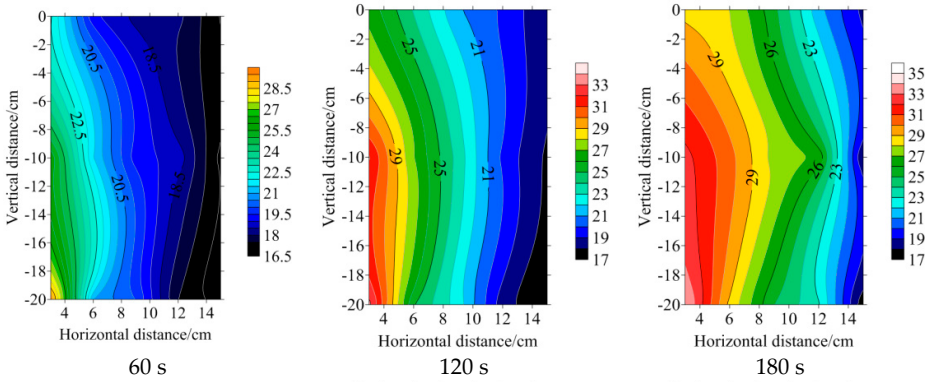
Vertical distance/cm
Horizontal distance/cm
60 s
120 s
180 s

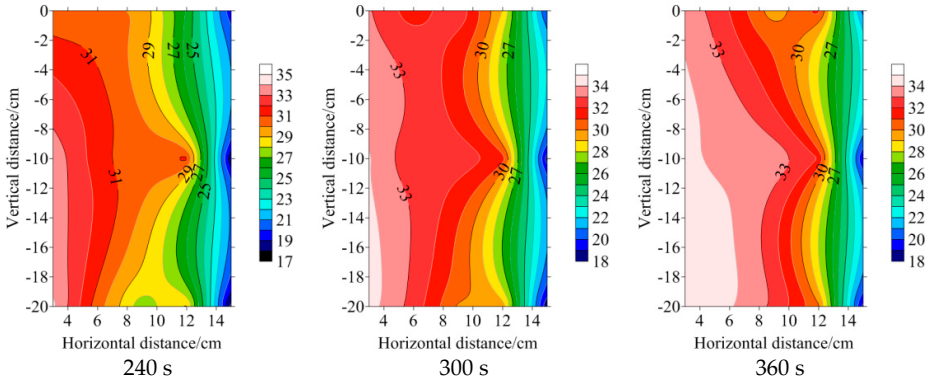
Vertical distance/cm
Horizontal distance/cm
240 s
300 s
360 s

(**b**)

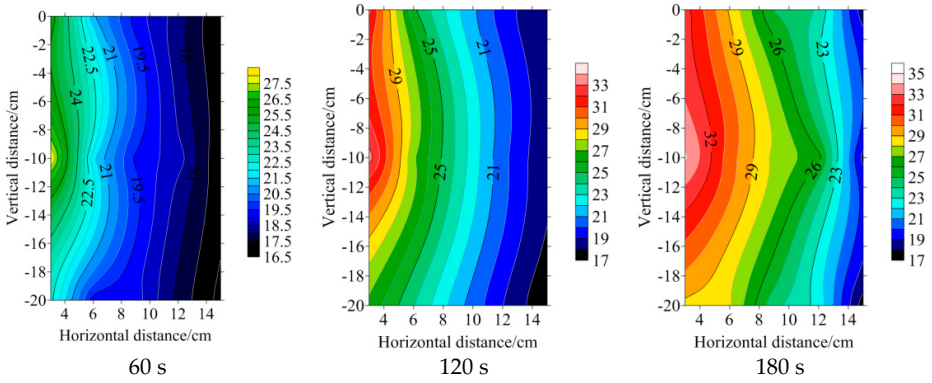
Vertical distance/cm
Horizontal distance/cm
60 s
120 s
180 s

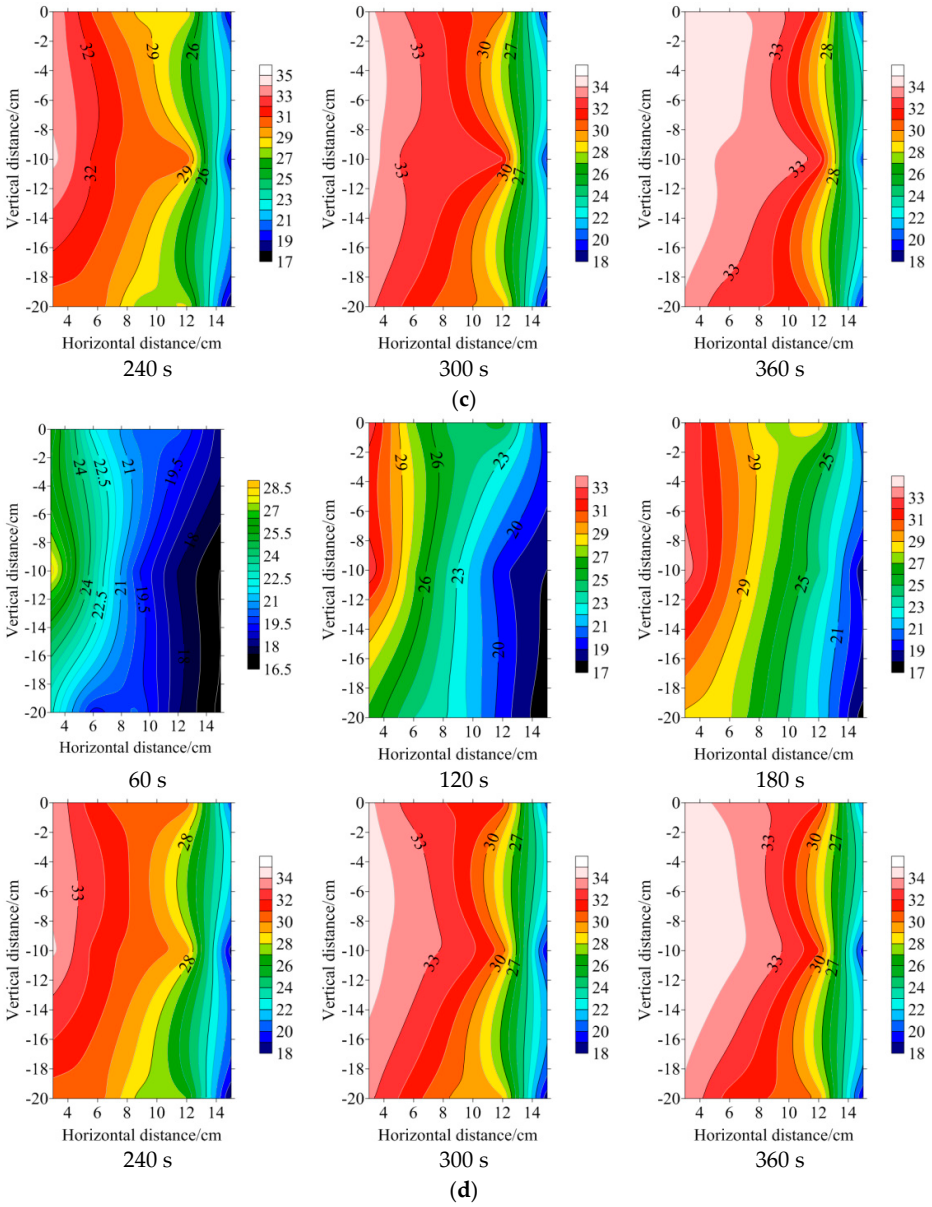

Figure 14. SWC distribution. (**a**) <2 mm; (**b**) 7–17 mm; (**c**) 17–27 mm; (**d**) >27 mm. Note: The legend is in SWC, %.

4.4. Energy Consumption Analysis

As shown in Table 7, the particle size has a significant effect on energy consumption, where the energy consumption for the particle size of 2 mm is 477 kJ and the energy consumption for the particle size of >27 mm is 486 kJ. The energy consumption for the particle sizes 7–17, 17–27, and >27 increased by 6.17%, 6.7%, and 9.4%, respectively, compared with that for a particle size of 2 mm. The effect of steam flow on the energy consumption is not significant.

Table 7. Energy consumption.

SP Size (mm)	Flow Rate (kg/h)	Energy Consumption (kJ)
<2	2	476.75 ± 1.33 ^{b}
	3	476.67 ± 1.30 ^{b}
	4	476.58 ± 1.37 ^{b}

	2	482.85 ± 1.6 [ab]
7–17	3	482.90 ± 1.59 [ab]
	4	482.77 ± 1.50 [ab]
	2	483.36 ± 2.79 [a]
17–27	3	483.28 ± 2.81 [a]
	4	483.45 ± 2.80 [a]
	2	486.17 ± 4.15 [a]
>27	3	485.60 ± 4.52 [a]
	4	486.35 ± 4.11 [a]

Note: The data are given as the mean ± standard deviation ($n = 3$); different lowercase letters indicate significant differences in the same flow rate ($p < 0.05$).

5. Discussion

Considering the characteristics of Yangtze River Delta soil and to promote the diffusion and heating range of steam in the soil disinfection process, the soil heating rate, temperature distribution, and energy consumption were analyzed by changing the particle and pore size of the soil. Results showed that with an increase in the SP size, the width of the soil pore flow channel gradually increased and the diffusion and the heating rate of steam in the vertical direction is greater than that in the horizontal direction, such that a large amount of steam will overflow the soil surface. Comparing the simulation and test results, it can be seen that the temperature field simulated by CFD is higher than the SSD test at the horizontal diffusion distance *L* and the temperature value. This is because the simulation condition is ideal and the heat dissipation is negligible, so the simulation value is greater than the test value. However, there may also be another reason. During the test, due to the continuous flow of steam into the soil, part of the steam will condense into water vapor and liquid water, and some soil particles will disintegrate and aggregate to form larger soil clods [28]. In the later stage of disinfection, the diffusion of steam in the soil will be hindered, which will reduce the diffusion range of the steam and the soil temperature value. Therefore, in future simulation processes, it is necessary to consider the problem of soil particle disintegration and deformation. At the same time, it is also necessary to simulate the impact of water content (steam condensate) changes on soil particles and temperature field during the simulation process.

Although the simulation value is higher than the experimental value, we can still find some new ones. The visualization of simulation process and verification of temperature field of disinfection test indicatedthat the SP size and pores have a substantial influence on the flow of steam. When the pores are too large, the steam primarily forms a large pore flow in the vertical direction and rapidly diffuses to the surface of the soil to form a high-temperature region [16,17]. A large amount of steam will overflow into the air to cause an ineffective loss of heat, and with a decrease in the SP size, the soil pore flow channel becomes fine and the diffusion velocity of steam in the vertical direction gradually decreases, such that it diffuses around the soil in the form of matrix flow and partial large pore flow. Therefore, appropriately increasing soil pores can help to accelerate the flow of gases and liquids in the soil via the aeration and water permeability of the soil, especially in the soil disinfection process, and promote the diffusion and heat transfer range of the steam. However, the excessive pores in the soil cause the steam to diffuse too quickly to the surface of the soil and overflow into the atmosphere and cause a heat loss such that large particles in the soil cannot be completely heated to the desired temperature [16,17]. Similar to the mobile SSD process, the SDP is continuously pulled to form cracks of different sizes in the soil. Most of the steam will be directly lost from the crack to the air in the form of large pore flow, and only a small part of the steam will be the substrate flow [7]. The form spreads to both sides of the soil, which prevents the total soil warming from satisfying the temperature required for disinfection, which explains why mobile steam disinfection cannot quickly heat the soil.

Injecting steam disinfection is applied to different soil types. In addition to accelerating the diffusion rate of the soil vapor, the large pore flow can also promote the re-evaporation of

condensed water in the pores, which is conducive to gas diffusion. However, this situation is only applicable in sandy loam soils due to the high sand content and relatively large soil pores, which facilitates the diffusion of steam. The findings of Gay et al. indicated that the single-SDP steam has a thermal radius of 15 cm [6]. However, in clay soil, the diffusion of steam in dense soil is difficult. As indicated in the study with a particle size of 2 mm, although the pores have a large pore flow, the maximum horizontal heat transfer distance of single-SDP steam is only 12 cm, which is less than the working distance of sandy loam. Considering that the soil in the Yangtze River Delta is clay or clay loam, when using conventional soil steam sterilizer to inject steam sterilization of compacted clay, there will be problems of difficult steam diffusion and too small effective disinfection area. On the basis of this study, the compacted soil containing large cracks is finely rotated into a loose and porous small-grained soil by adding a rotary tillage device. The combined effects of large-pore steam flow and matrix flow after rotary tillage are more conducive to improving the effective disinfection range of steam. At the same time, according to the heat flow diffusion distance (12cm) of a single-SDP, it can be determined that the SDP spacing needs to be less than 24cm. In summary, it can be seen that the soil steam disinfection method will have a better practical disinfection effect than other disinfection methods after the rotary tilling treatment and the optimization of the SDP spacing.

6. Conclusions

Based on our findings following conclusions are drawn:

(1) For the clay soil in the Yangtze River Delta region of China, when the heat flow reaches H=20cm in the vertical direction, the simulation and test result of the heat flow in the maximum horizontal diffusion distance of single-SDP steam are L=13cm and 12cm, respectively. The test results are basically consistent with the simulation results. At the same disinfection time, the simulated soil temperature change trend is basically consistent with the test results and the test temperature is slightly lower than the simulated temperature. In the future, it is necessary to optimize the CFD simulation process, and add the disintegration and deformation processes of soil particle size with the change of water content.

(2) The larger the soil particle size is, the larger the pore flow path width, and the easier the formation of a large pore flow. Therefore, a large amount of steam will overflow into the air to cause an increase in energy consumption. In the future, it is necessary to add a rotary cultivating device to the soil steam sterilizer to rotate the soil to ensure that the soil can be heated uniformly and quickly.

Author Contributions: conceptualization, Z.Y.; methodology, Z.Y.; software, Z.Y.; validation, Z.Y., X.W., and M.A.; formal analysis, Z.Y.; data curation, Z.Y.; writing—original draft preparation, Z.Y. and A.A.; writing—review and editing, A.A. M.A., S.A.S., and H.Y.; visualization, A.A. M.A., S.A.S., and H.Y.; supervision, X.W.; project administration, X.W.; funding acquisition, X.W. and Z.Y. All authors have read and agreed to the published version of the manuscript.

Funding: This research was funded by the Jiangsu Province Science and Technology Support Plan-funded project CX(16)1002 and the Graduate Student Scientific Research Innovation Projects in Jiangsu Province KYCX17_0648.

Acknowledgments: We thank Hongyou Sun and Gang Li for helping with the work.

Conflicts of Interest: The authors declare no conflicts of interest.

SSD	soil steam disinfection
SP	soil particle
SDP	steam disinfection pipe
ST	soil temperature (°C)
SWC	soil water content (%)
Q_s	total amount of steam(kg)
Cv	coefficient of variation
V_T	soil temperaturerise rate(°C/s)

Ws energy consumption
L horizontal diffusion distance of the steam heat flow (cm)
H vertical diffusion distance of the steam heat flow (cm)
Subscripts
T temperature
s Steam
t time (s)

References

1. Weiland, J.E.; Littke, W.R.; Browning, J.E.; Edmonds, R.L.; Davis, A.; Beck, B.R.; Miller, T.W. Efficacy of reduced rate fumigant alternatives and methyl bromide against soilborne pathogens and weeds in western forest nurseries. *Crop Prot.* **2016**, *85*, 57–64, doi:10.1016/j.cropro.2016.03.016.
2. Yang, Y.T.; Hu, G.; Zhao, Q.L.; Guo, D.Q.; Gao, Q.S.; Guan, C.S. Research progress of soil physical disinfection equipment. *Agric. Eng.* **2015**, *5*, 43–48.(In Chinese)
3. Cao, A.; Zheng, J.; Wang, Q.; Li, Y.; Yan, D. Advances in soil disinfection technology worldwide. *China Veg.* **2010**, *21*, 17–22. (In Chinese)
4. Cao, A.; Zheng, J.; Guo, M.; Wang, Q.; Li, Y. Soil disinfection technology and key points. *Vegetables***2011**,*4*, 41–44. (In Chinese)
5. Nishimura, A.; Asai, M.; Shibuya, T.; Kurokawa, S.; Nakamura, H. A steaming method for killing weed seeds produced in the current year under untilled conditions. *Crop Prot.***2015**, *71*, 125–131, doi:10.1016/j.cropro.2015.02.015.
6. Gay, P.; Piccarolo, P.; Aimonino, D.R.; Tortia, C. A high efficiency steam soil disinfestation system, Part I: Physical background and steam supply optimisation. *Biosyst. Eng.***2010**, *107*, 74–85, doi:10.1016/j.biosystemseng.2010.07.003.
7. Gay, P.; Piccarolo, P.; Aimonino, D.R.; Tortia, C. A high efficiency steam soil disinfestation system, part II: Design and testing. *Biosyst. Eng.***2010**, *107*, 194–201, doi:10.1016/j.biosystemseng.2010.07.008.
8. Peruzzi, A.; Raffaelli, M.; Ginanni, M.; Fontanelli, M.; Frasconi, C. An innovative self-propelled machine for soil disinfection using steam and chemicals in an exothermic reaction. *Biosyst. Eng.***2011**, *110*, 434–442, doi:10.1016/j.biosystemseng.2011.09.008.
9. Pan, S.P.; Zhou, H.P.; Jiang, X.S.; Chen, Q.; Li, P.P. Design and experiment of soil disinfection steam generator based on pulse combustion technology. *Trans. Chin. Soc. Agric. Mach.* **2018**,*49*, 301–307. (In Chinese)
10. Xu, Y.L.; Dai, L.; Zhao, D.; Zhang, Y.J.; Jin, B.H.; Zhang, X.D.; He, X.H. Effect of several soil treatments on seedling growth and root rot disease of *Panax notoginsen*. *J. Yunnan Agric. Univ.* **2016**,*31*, 1006–1011. (In Chinese)
11. Zhu, J.F.; Zhao, Y.Q.; Yang, L.Q.; Gao, Z.C.; Zhang, R.K. Design of matrix steam sterilizing machine of Panax Notoginseng greenhouse seedling trough. *J. Agric. Mech. Res.* **2017**,*3*, 79–83. (In Chinese)
12. Huang, C.Y. *Soil Science*; China Agriculture Press: Beijing, China, 2000; pp. 71–78.
13. Lin, D.Y. *Soil Science*; China Forestry Press: Beijing, China, 2002; pp. 61–66.
14. Li, D.C.;Zhang, T.L. Fractal features of particle size distribution of soils in China. *Soil Environ. Sci.***2000**, *9*, 263–265.(In Chinese)
15. Ding, R.X.;Liu, Y.Z.; Sun, Y.H. Reference of soil system classification in subtropical humid region of China. *Soils***1999**,*2*, 97–109, doi:10.13758/j.cnki.tr.1999.02.007. (In Chinese)
16. Skopp, J.; Gardner, W.R.; Tyler, E.J. Solute movement in structured Soils: Two-region model with small interaction. *Soil Sci. Soc. Am. J.* **1981**,*45*, 837–842.
17. Hardie, M.A.; Marcus, A.; Cotching, W.E.;Holz, G.; Lisson, S.; Mattern, K. Effect of antecedent soil moisture on preferential flow in a texture-contrast soil. *J. Hydrol.* **2011**,*398*, 191–201.
18. Ameen, M.; Xiaochan, W.; Yaseen, M.; Umair, M.; Yousaf, K.; Yang, Z.; Soomro, S.A. Performance Evaluationof Root Zone Heating System Developed with Sustainable Materials for Application in Low Temperatures.*Sustainability***2018**,*10*, 4130.
19. Beven, K.; Germann, P. Water flow in soil macropores II. A combined flow model. *Eur. J. Soil Sci.* **1981**, *32*,15–29.
20. Beven, K.; Germann, P. Macropores and water flow in soils. *Water Resour. Res.* **1982**,*18*, 1311–1325.
21. Luxmoore, R.J. Micro-, Meso-, and Macroporosity of soil. *Soil Sci. Soc.Am. J.* **1981**,*45*, 671–672.

22. Wilson, G.V.; Luxmoore, R.J. Infiltration, Macroporosity, and Mesoporosity distributions on two forested watersheds. *Soil Sci. Soc.Am. J.* **1988**,*52*, 329–335.
23. Singh, P.; Kanwar, R.S.; Thompson, M.L. Measurement and Characterization of Macropores by using Autocad and Automatic Image Analysis. *J. Environ. Qual.* **1991**,*20*, 289–294.
24. Soille, P.J.; Ansoult, M.M. Automated basin delineation from digital elevation models using mathematical morphology. *Signal Process.* **1990**,*20*, 171–182.
25. El-Halim, A. Image processing technique to assess the use of sugarcane pith to mitigate clayey soil cracks: Laboratory experiment. *Soil Tillage Res.* **2017**,*169*, 138–145.
26. Wang, C.; Zhang, Z.Y.; Liu, Y.; Fan, S.M. Geometric and fractal analysis of dynamic cracking patterns subjected to wetting-drying cycles. *Soil Tillage Res.* **2017**,*170*, 1–13.
27. Yang, Z.J.; Wang, X.C.; Ameen, M. Influence of the spacing of steam-injecting pipes on the energy consumption and soil temperature field for clay-Loam disinfection. *Energies***2019**,*12*, 3209.
28. Li, Q.; Zhang, Z.; Xu, H.; Xu, W.Z. Anew modified method for calculation of soil disintegration rate. *Res. SoilWater Conserv.* **2015**,*22*, 344–348.